Global properties of circumgalactic medium at high-redshift: spectroscopic study of strong Lyman-α forest absorbers

Debopam Som

Laboratoire d'**A**strophysique de **M**arseille/Aix-Marseille Université

with: Matthew Pieri et al.

LAM LABORATOIRE D'ASTROPHYSIQUE DE MARSEILLE

Intergalactic Interconnections Marseille

10th July 2018

A*Midex Initiative d'excellence Aix-Marseille

Quasar

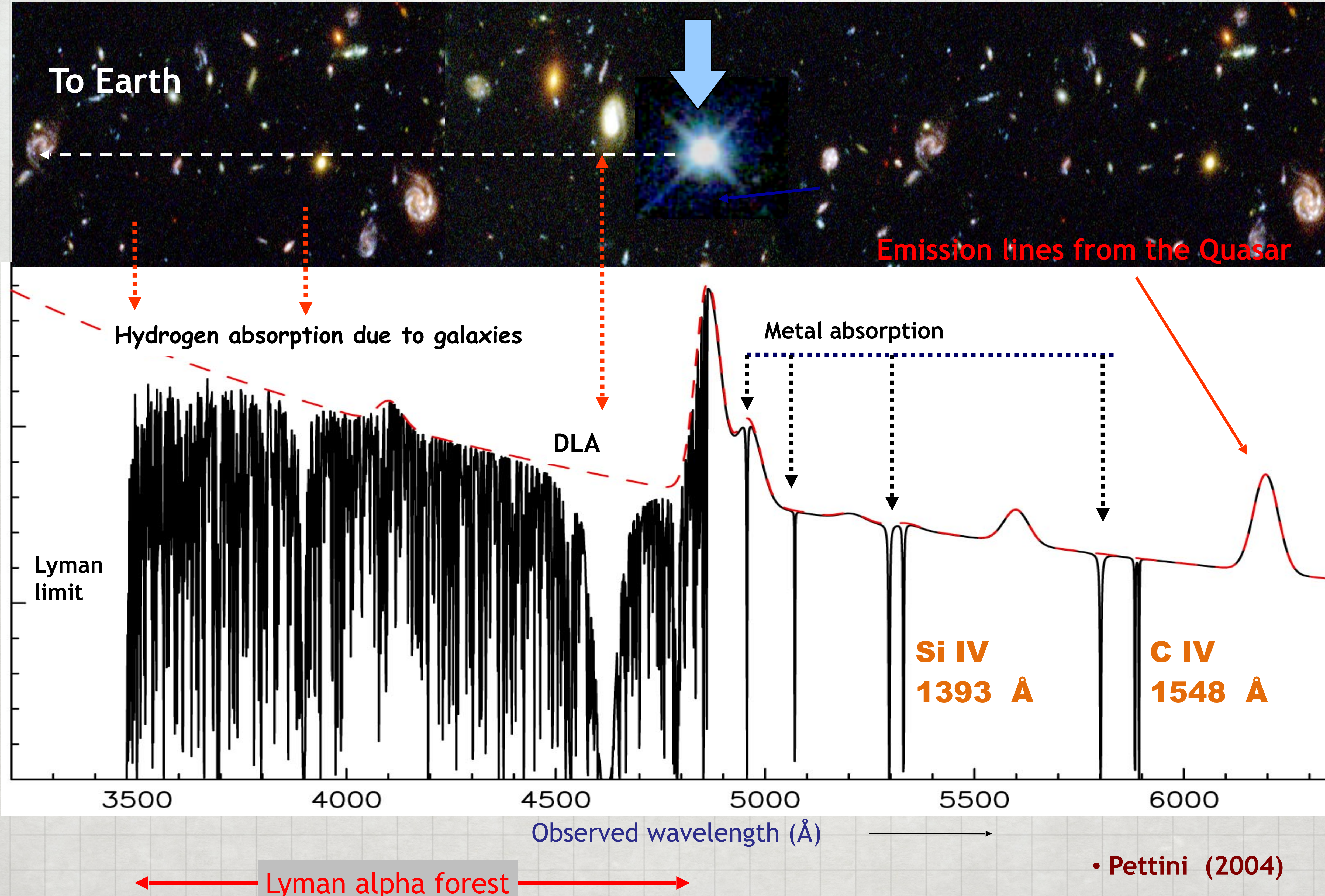

• Pettini (2004)

Different QSO absorbers:

- Lyman-α forest: N(HI) < $10^{17.2}$ cm^{-2}.
- Lyman Limit systems: $10^{17.2}$ cm^{-2} < N(HI) < 10^{19} cm^{-2} .
- Sub-damped Ly-α systems (sub-DLAs):
  10^{19} cm^{-2} < N(HI) < $10^{20.3}$ cm^{-2} .
- Damped Ly-α systems (DLAs): N(HI) > $10^{20.3}$ cm^{-2} .

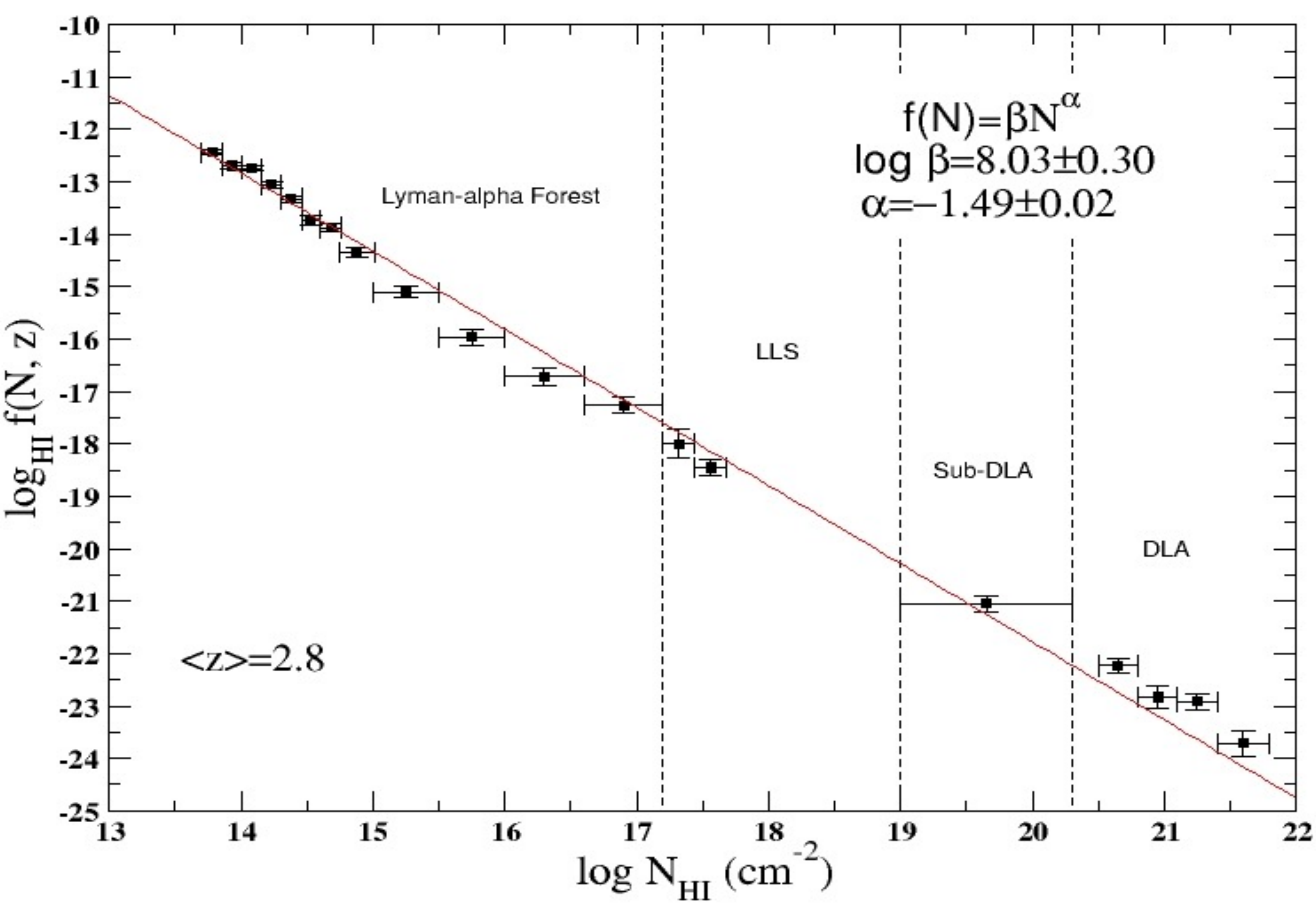

f(N)=βN^α
log β=8.03±0.30
α=−1.49±0.02
Lyman-alpha Forest
LLS
Sub-DLA
DLA
<z>=2.8
log_HI f(N, z)
log N_HI (cm^-2)
-10
-11
-12
-13
-14
-15
-16
-17
-18
-19
-20
-21
-22
-23
-24
-25
13
14
15
16
17
18
19
20
21
22

BLENDED HI AS A PROXY FOR CGM

- **Lyman α absorbers around galaxies are blended on SDSS resolution scales (Rakic et al. 2012, Turner et al 2014) ...**

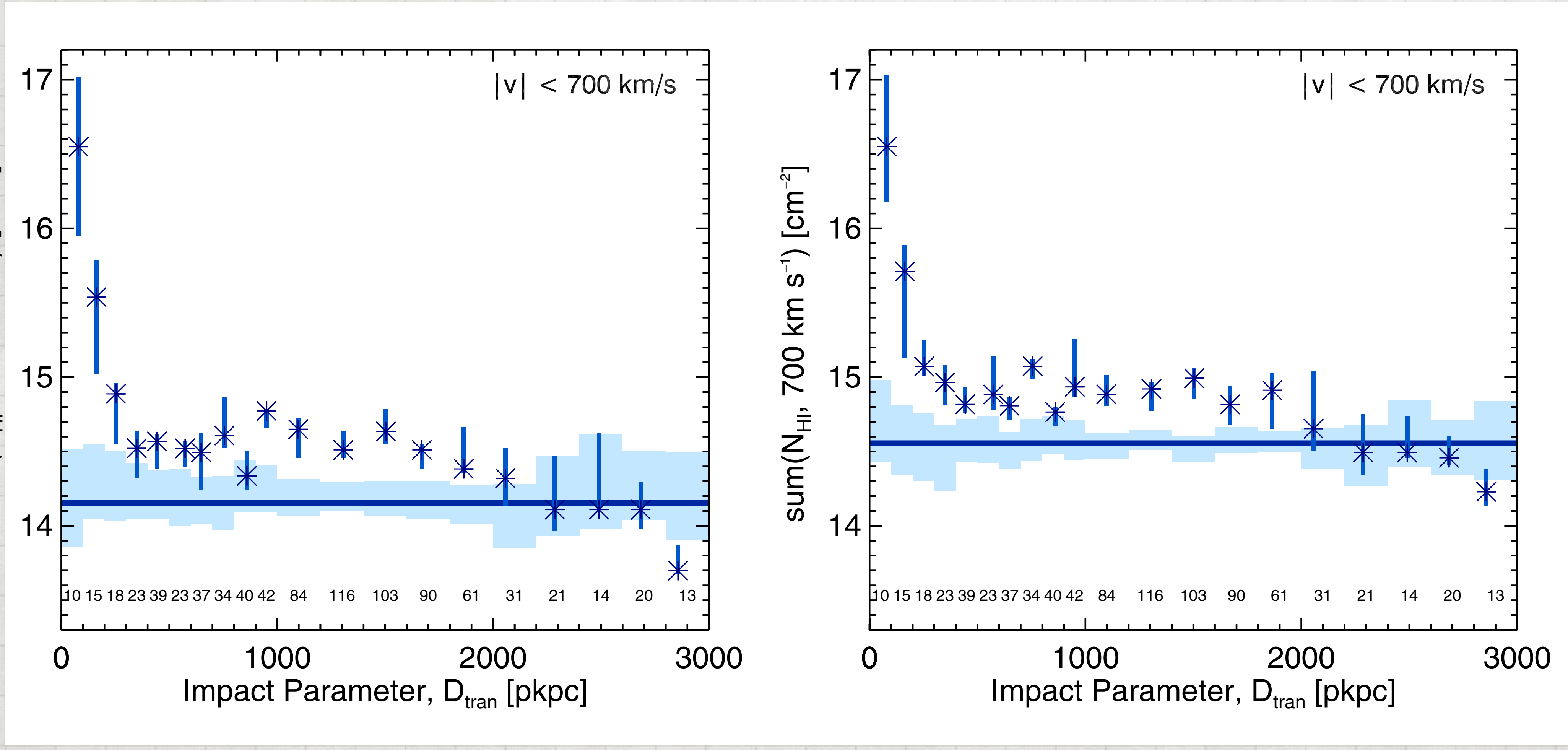

... have $10^{14.5}$<N_{HI}<$10^{16.5}$ 100-300 kpc scales (Rudie et al. 2012) ...

‘strong’=‘blended’

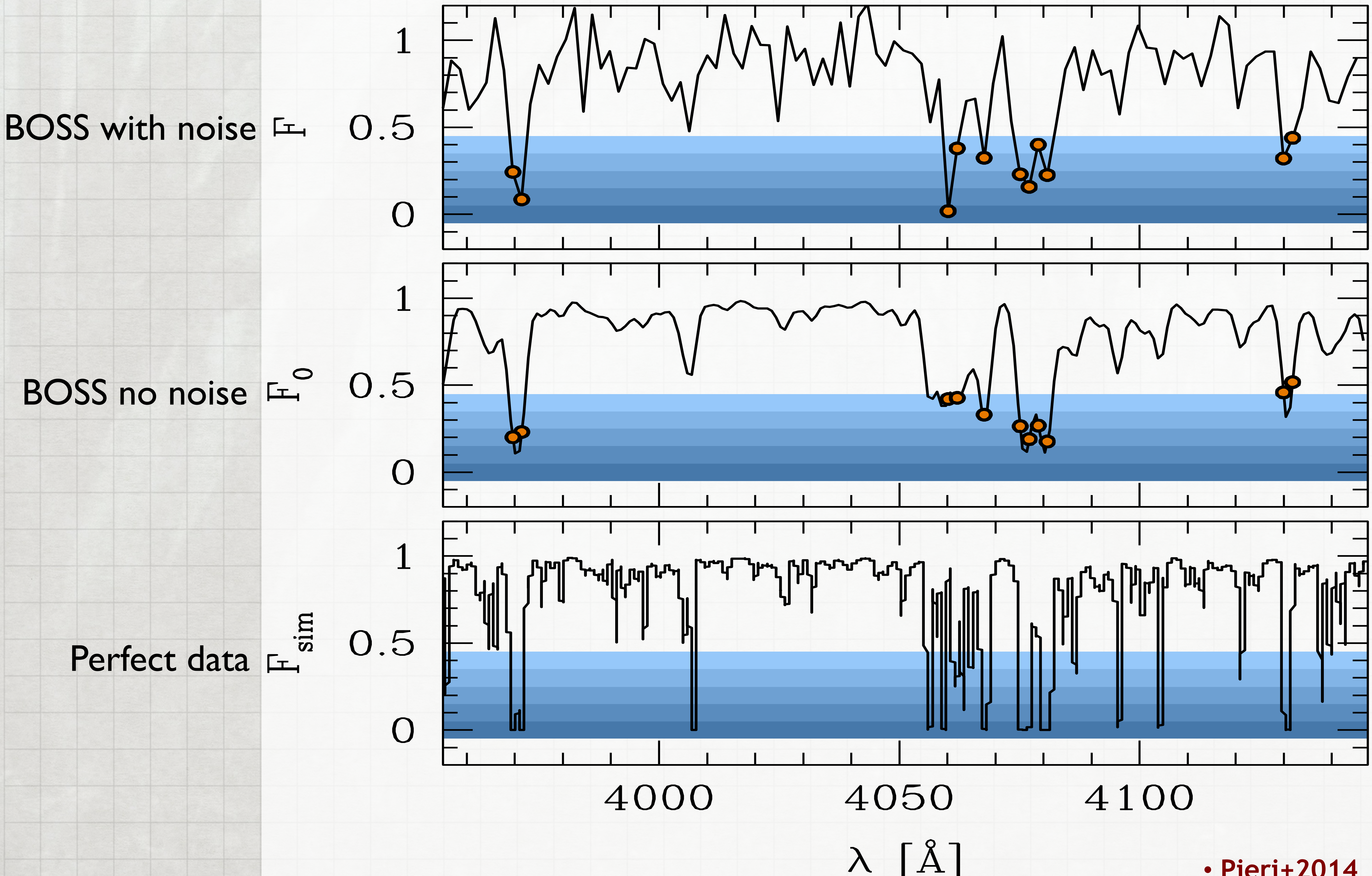

• Pieri+2014

Galaxies (identified) in Absorption

- **LBGs near bright quasar sightlines: VLT LBGs (Crighton et al 2011), subset of KBSS (Rudie et al 2012)**
- **Compare by matching BOSS resolution and binning**

Rudie et al. (2012) working definition

"near galaxies" = CGM

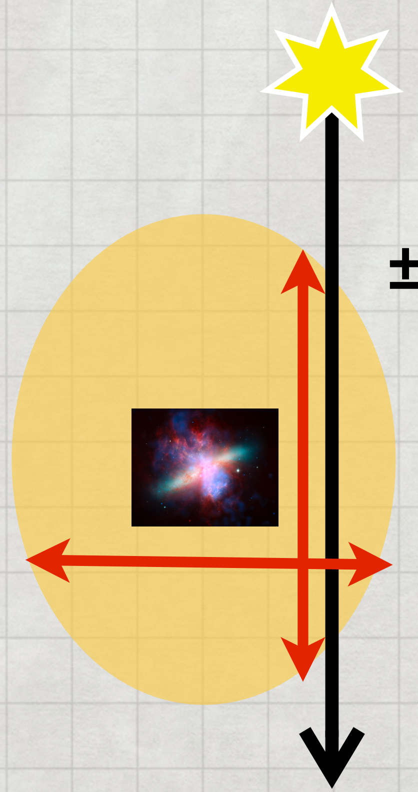

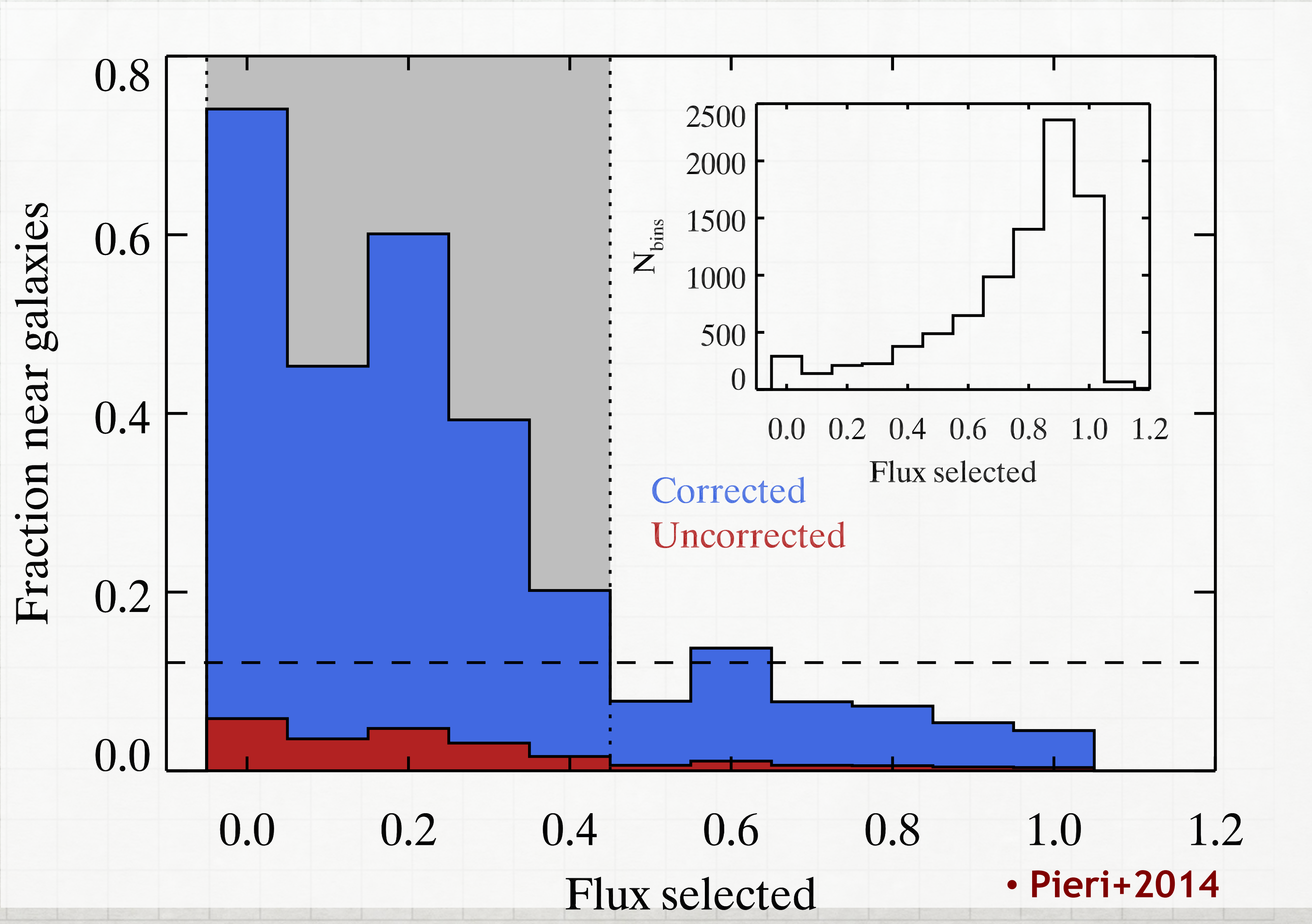

• Pieri+2014

Galaxies (identified) in Absorption

- **Cross-correlating the strong Lyman-α sample with SDSS DR14 (eBOSS) Lyman-α forest indicates bias ~ 2 (more in the talk by Michael Blomqvist)**

Rudie et al. (2012) working definition

"near galaxies" = CGM

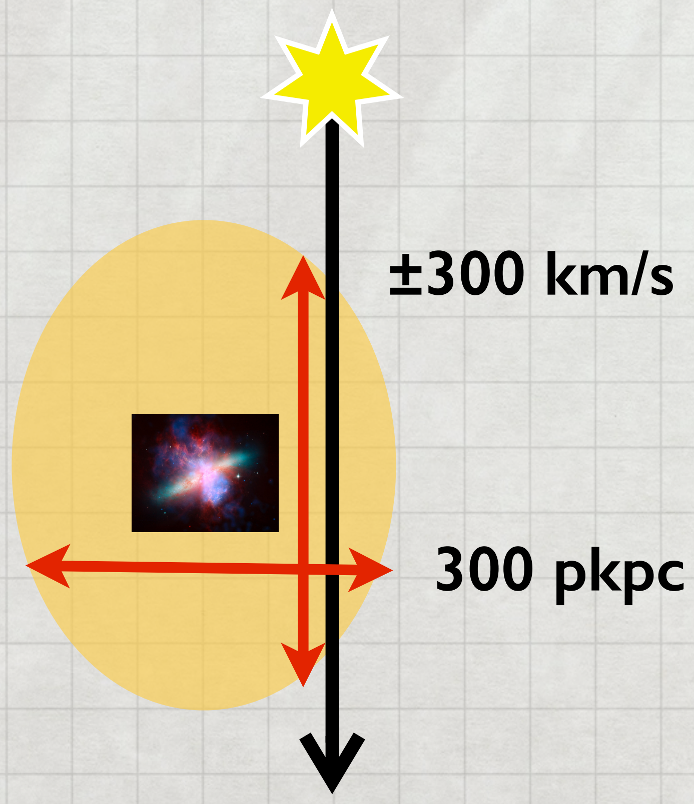

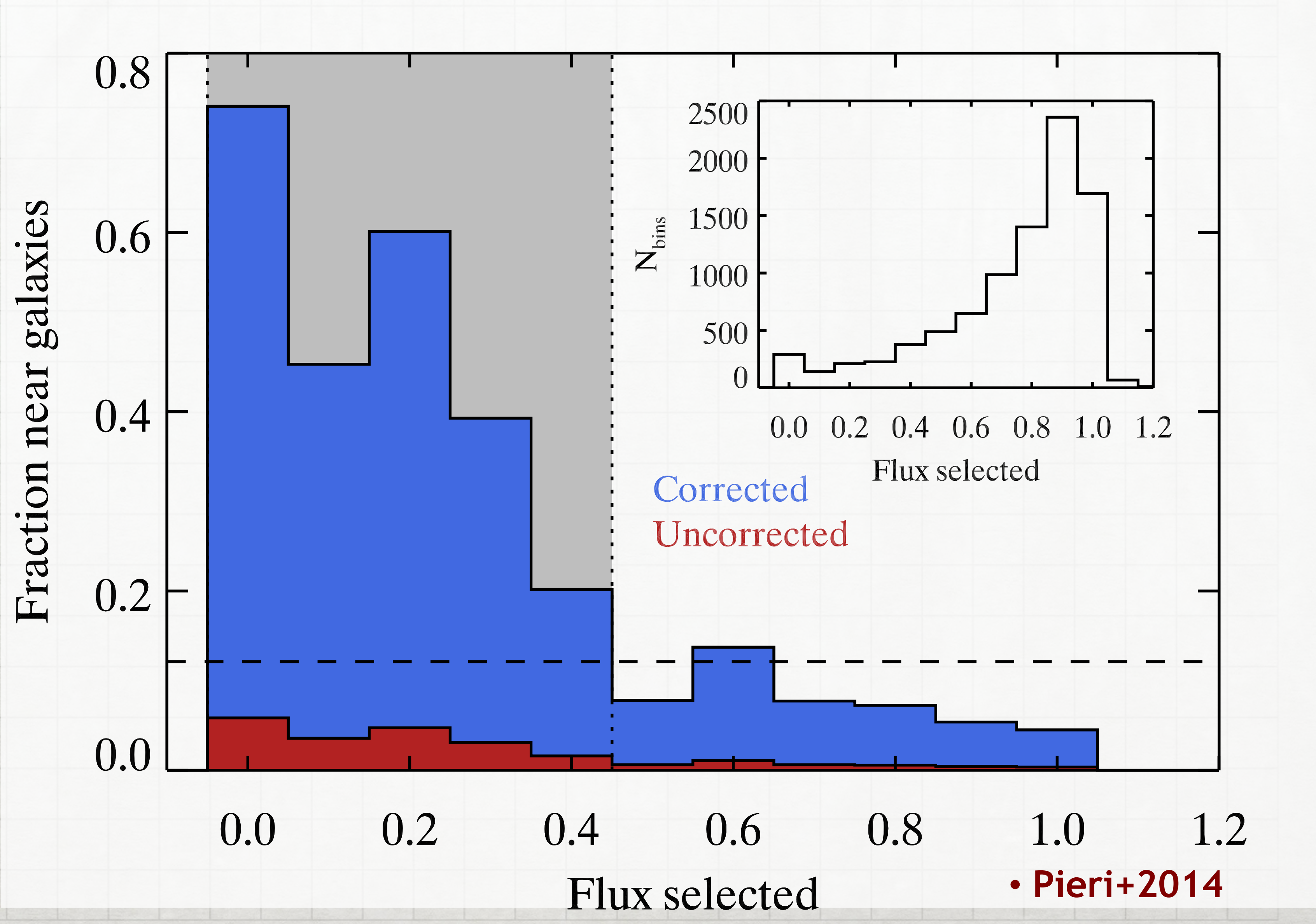

• Pieri+2014

Baryon Oscillation Spectroscopic Survey

- 1 of 4 in SDSS-III 2009-2014
- 10k deg^2
- Goal: 1.6M galaxies and ~160k forest quasars
- Resolution R = 2000

2<z<3.4 forest

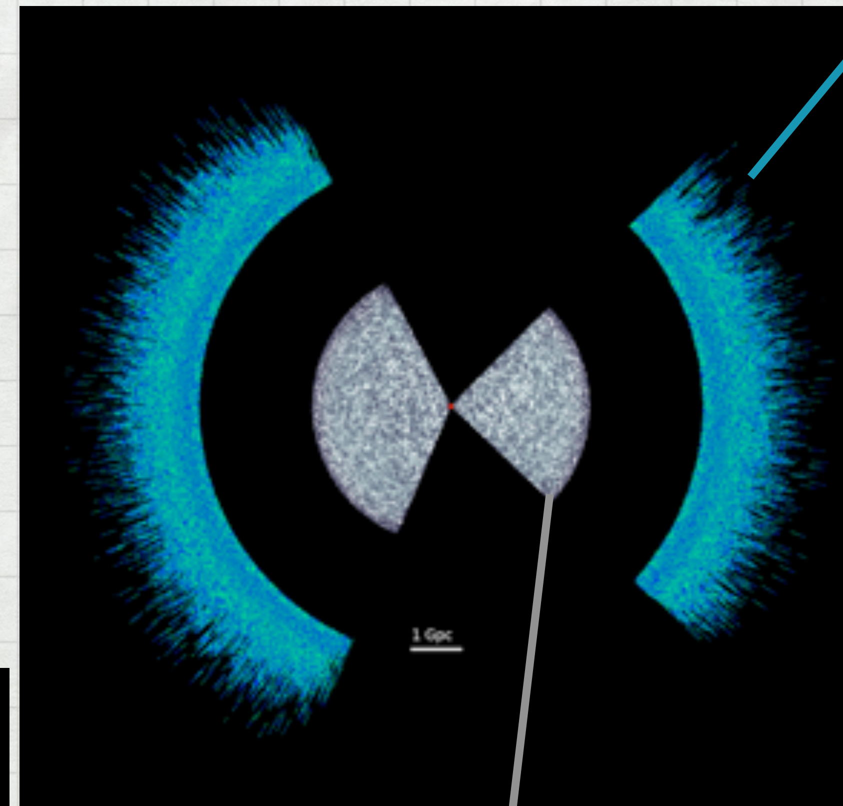

z<0.7 galaxies

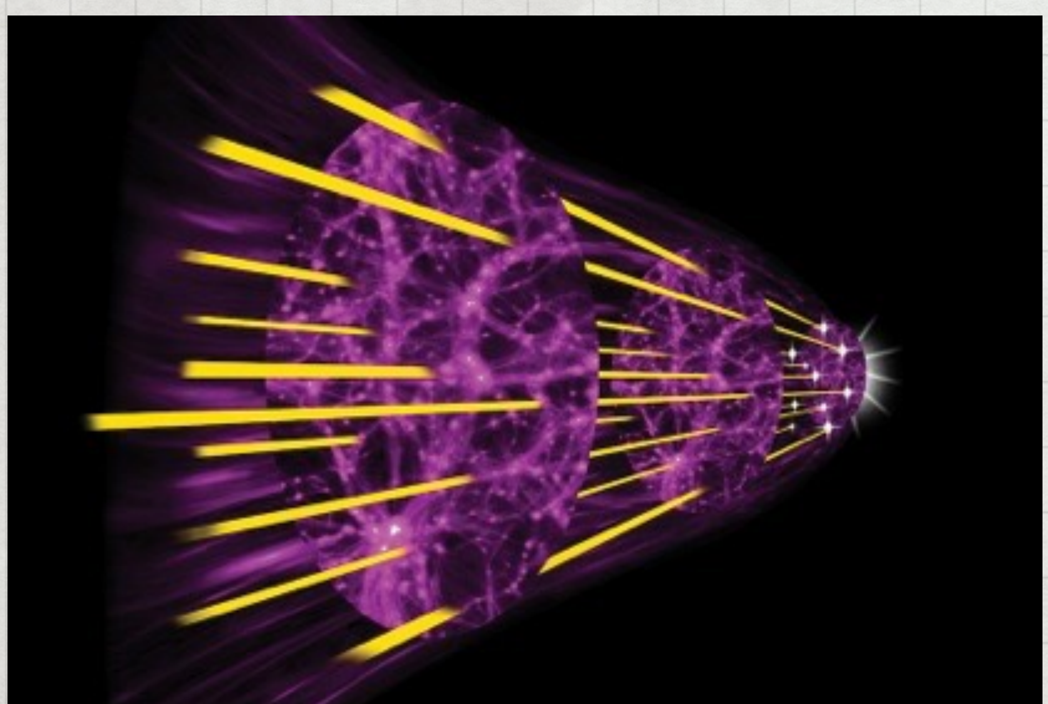

DR12 with 158k QSOs

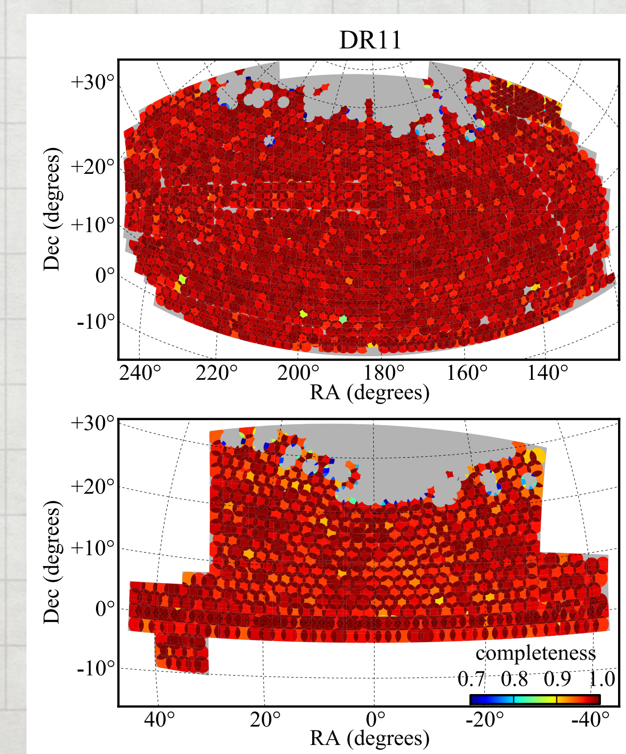

Stacking Lyman α Forest Absorbers

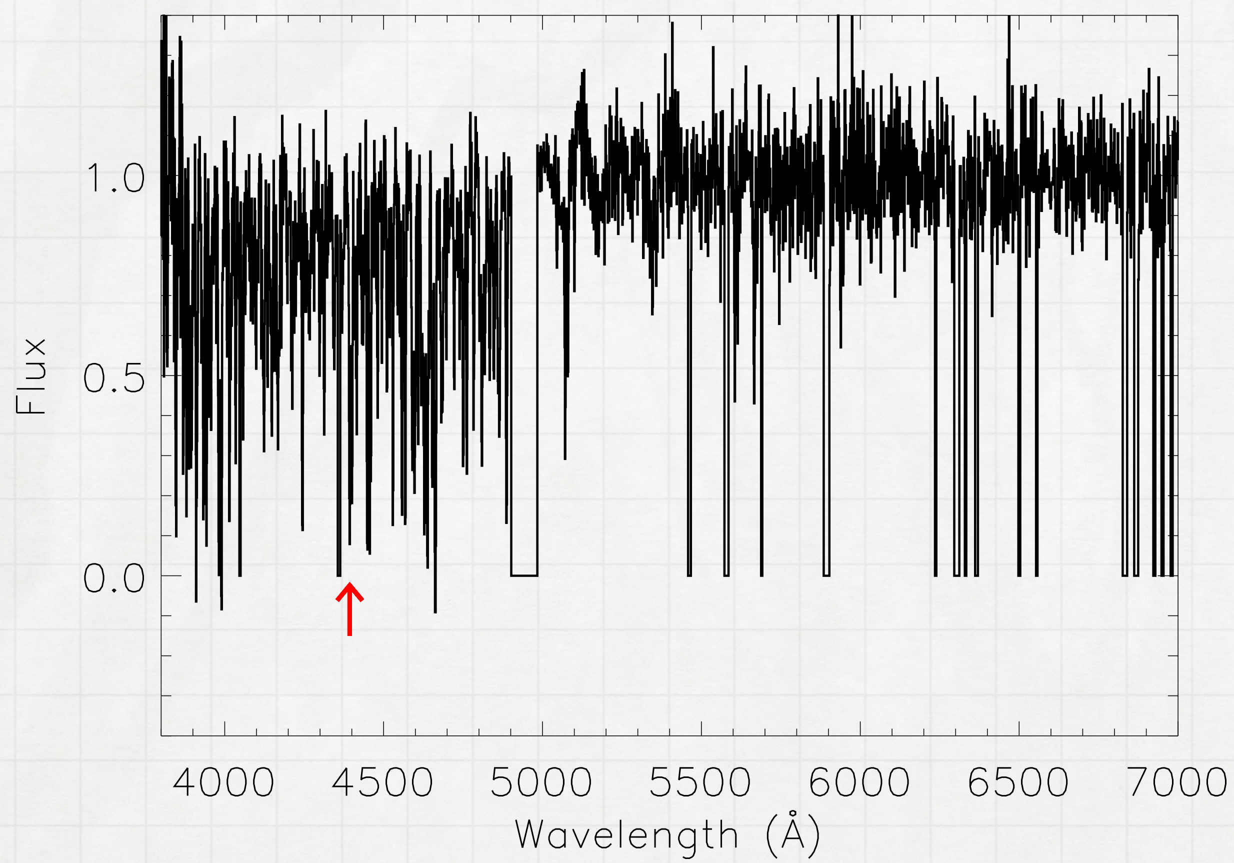

The entire spectrum shifted to the rest-frame of the Lyman α forest absorber of interest and stacked to see any metals available

(Pieri+ 2010b; SDSS II data)

Composite spectrum of Lyman α forest absorbers

Stacking Lyman α Forest Absorbers

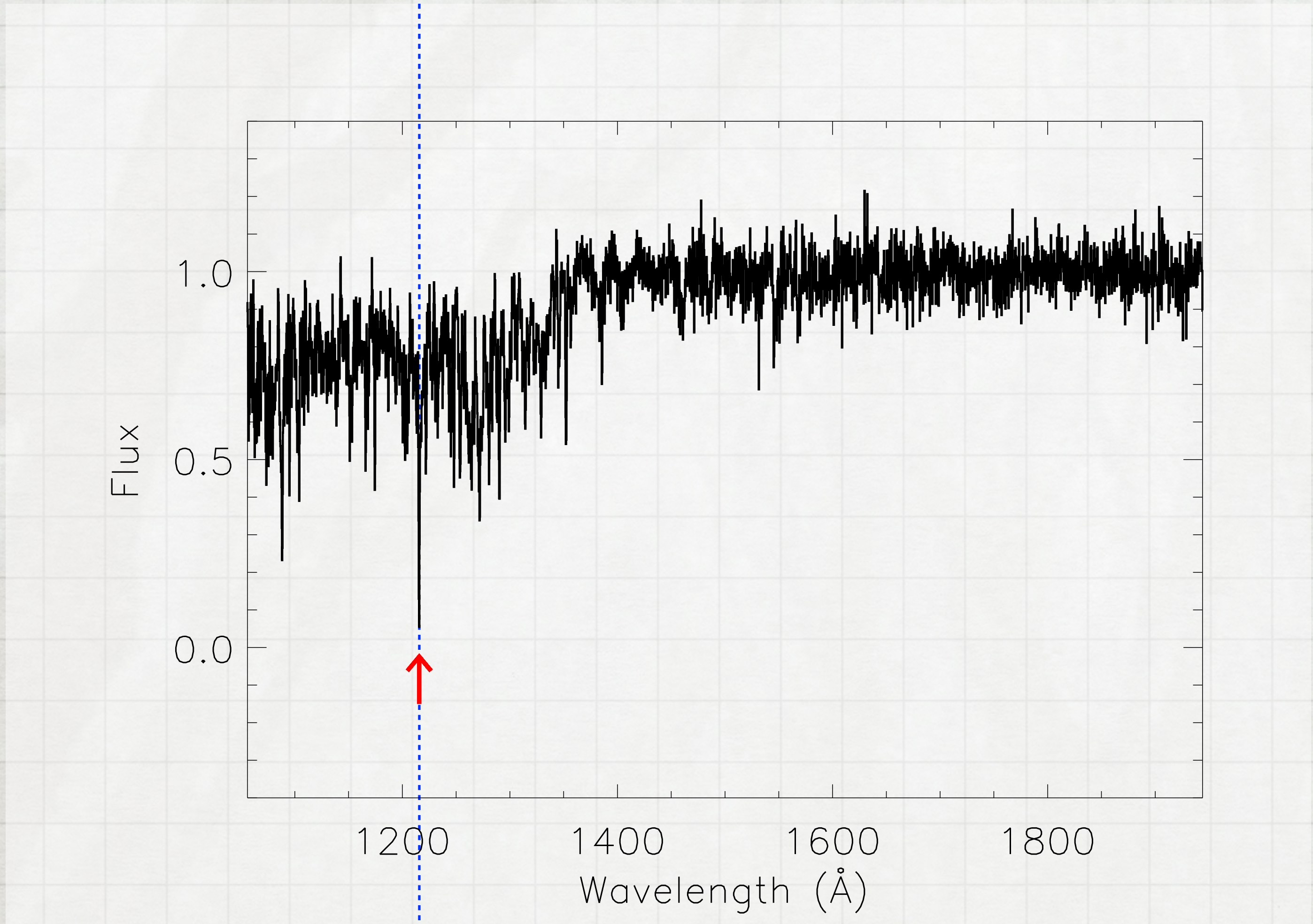

The entire spectrum shifted to the rest-frame of the Lyman α forest absorber of interest and stacked to see any metals available

(Pieri+ 2010b; SDSS II data)

Composite spectrum of Lyman α forest absorbers

Stacking Lyman α Forest Absorbers

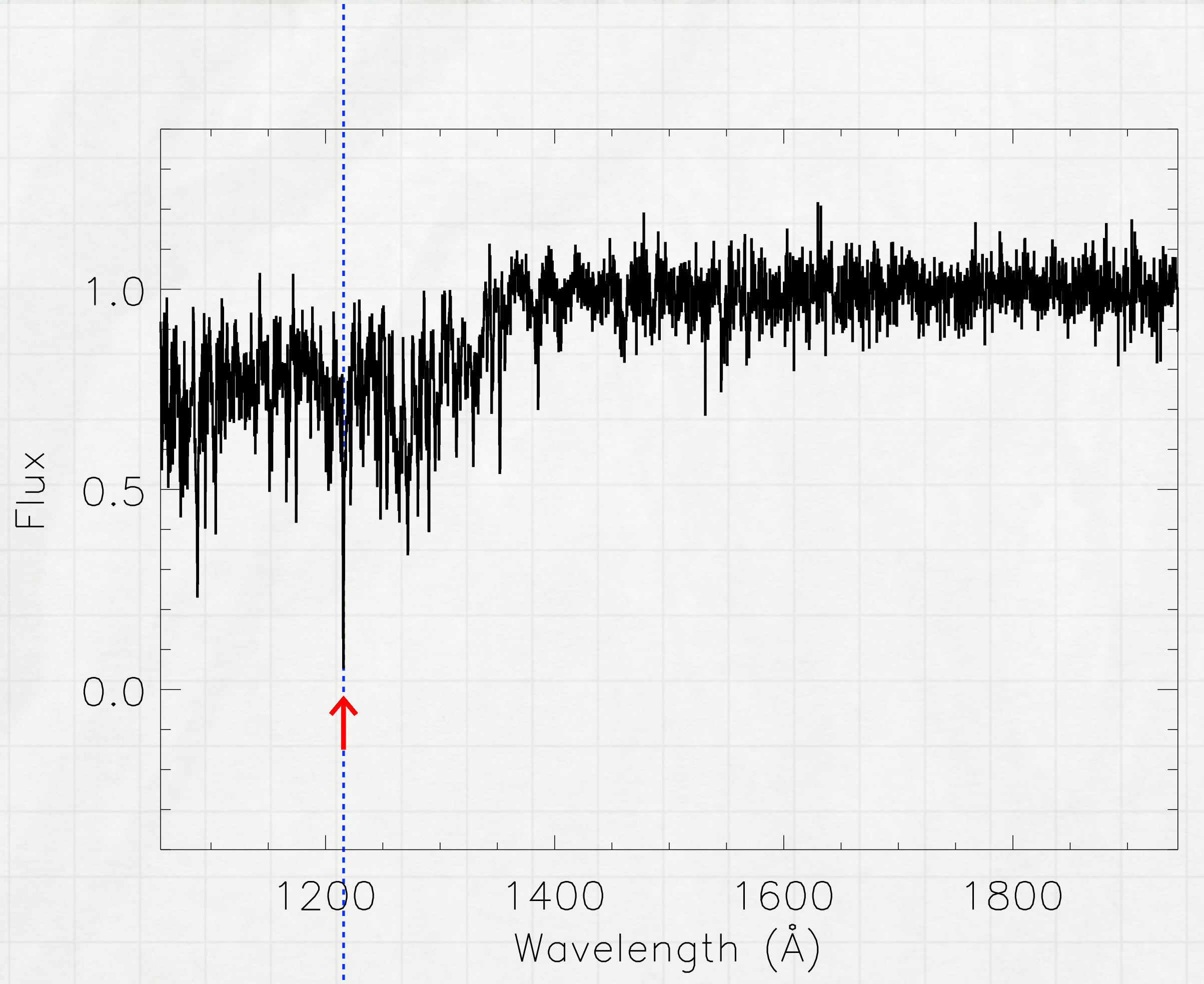

The entire spectrum shifted to the rest-frame of the Lyman α forest absorber of interest and stacked to see any metals available

(Pieri+ 2010b; SDSS II data)

Composite spectrum of Lyman α forest absorbers

Stacking Lyman α Forest Absorbers

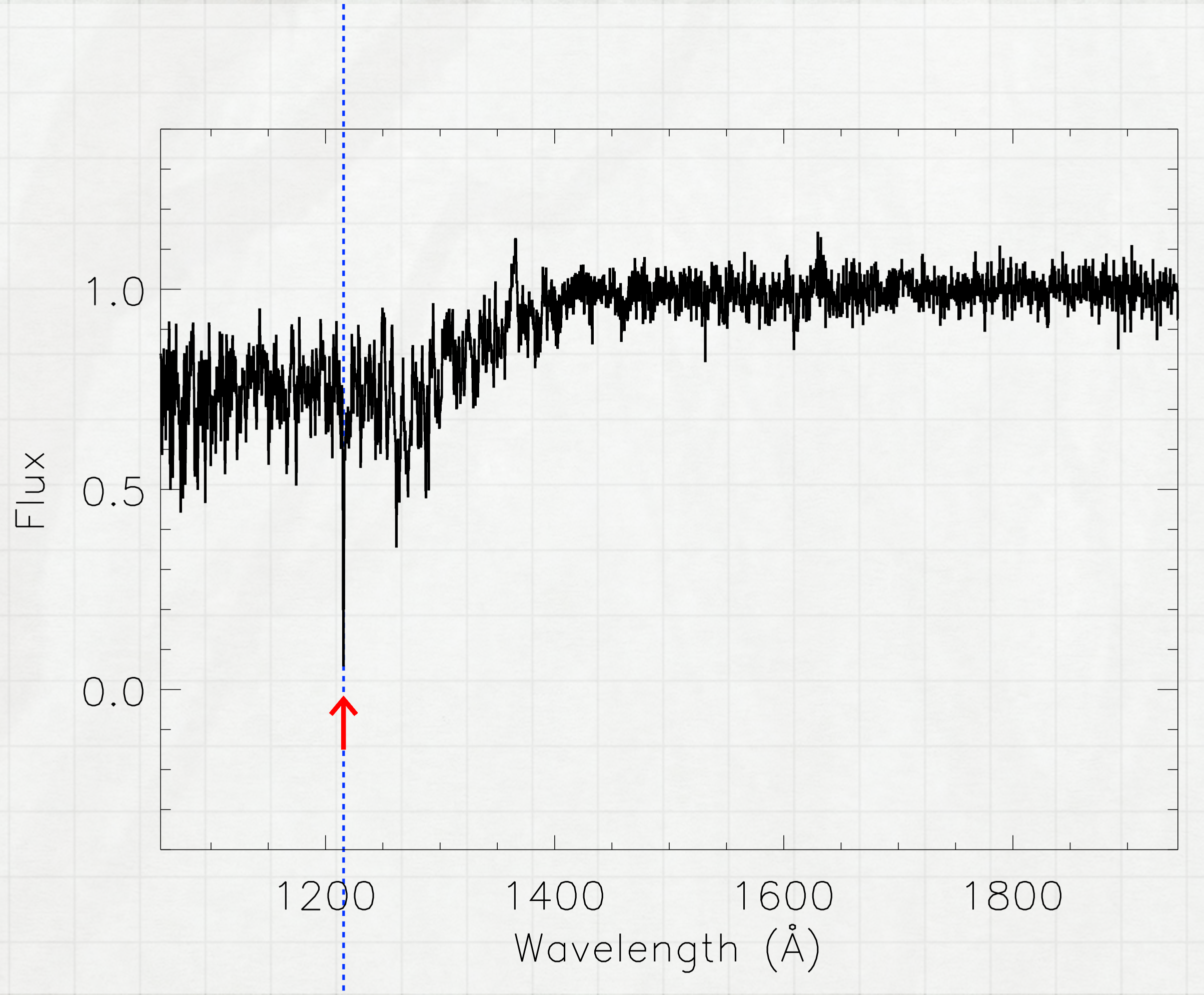

The entire spectrum shifted to the rest-frame of the Lyman α forest absorber of interest and stacked to see any metals available

(Pieri+ 2010b; SDSS II data)

Composite spectrum of Lyman α forest absorbers

Composite Spectrum of Lyman α Forest Absorbers using BOSS Quasars

Lyα absorbers @ 2.4<z<3.1

Complete DR12 Sample

Multiple lines/elements/ions - breaking degeneracies:

- physical conditions of gas
- abundance patterns
- UV background shape, intensity

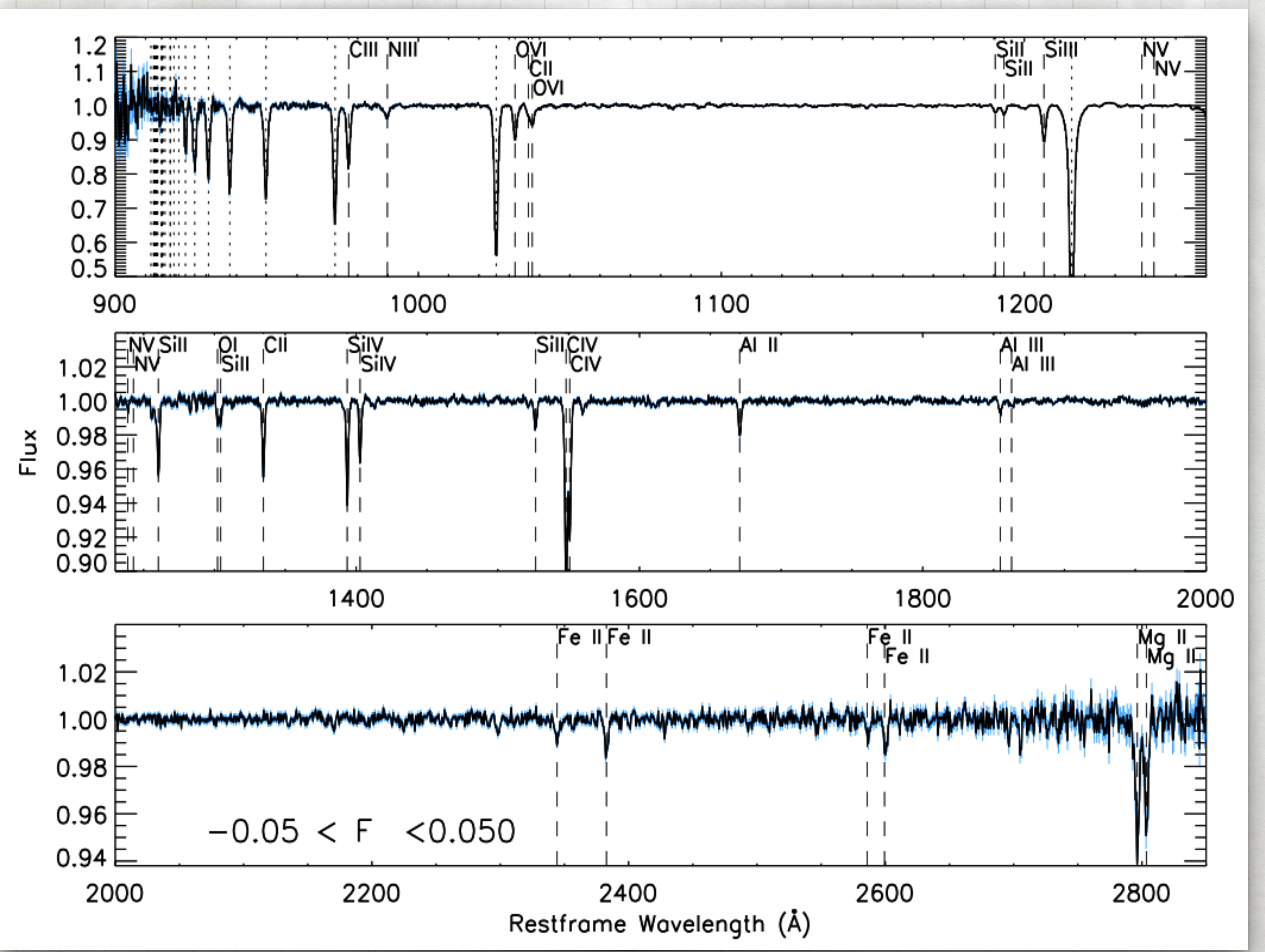

• Som, Pieri et al., in prep.

Composite Spectrum of Lyman α Forest Absorbers using BOSS Quasars

Lyα absorbers @ 2.4<z<3.1

Complete DR12 Sample

Multiple lines/ elements/ions - breaking degeneracies:

- physical conditions of gas
- abundance patterns
- UV background shape, intensity

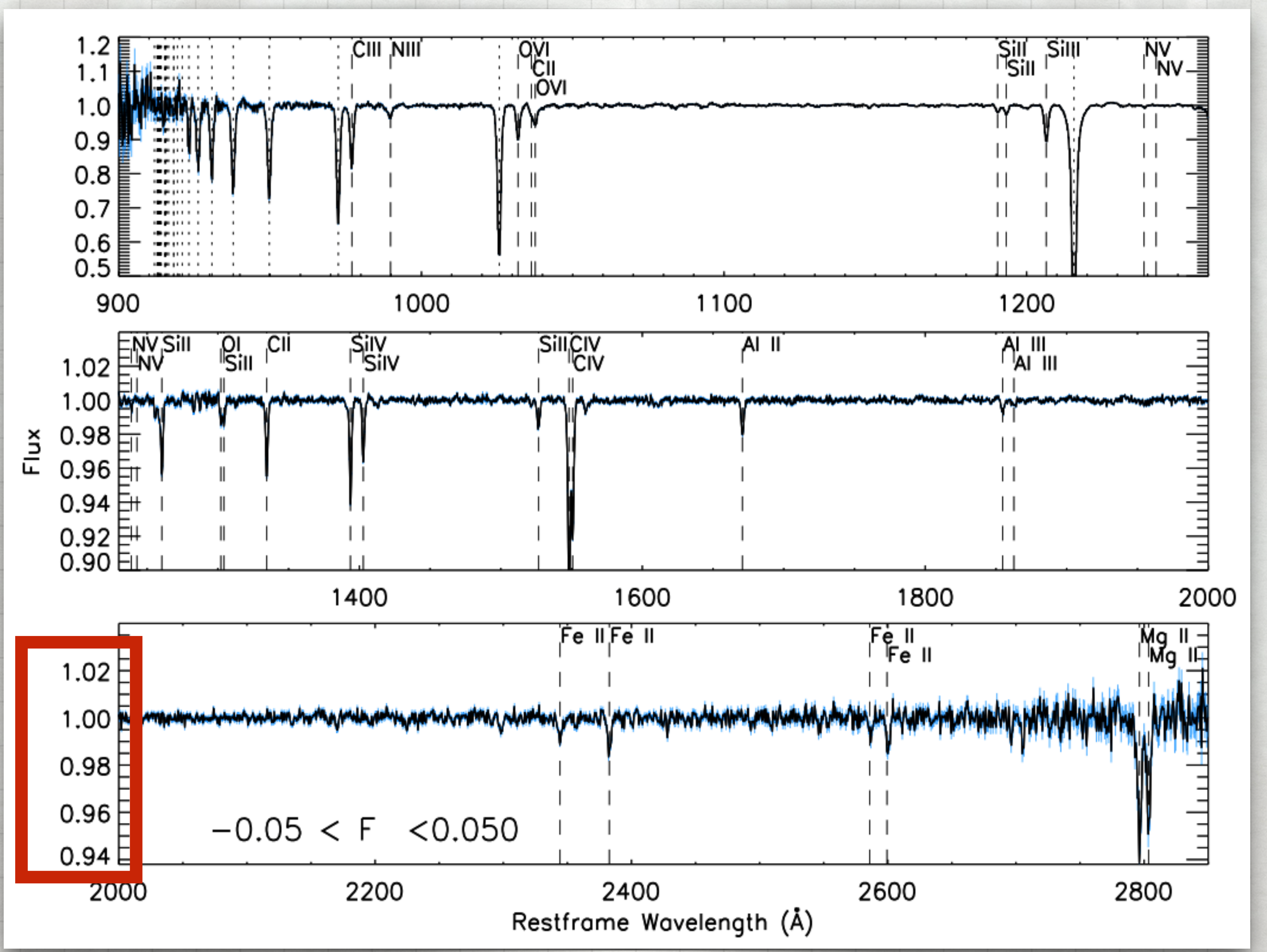

• Som, Pieri et al., in prep.

What do we get?

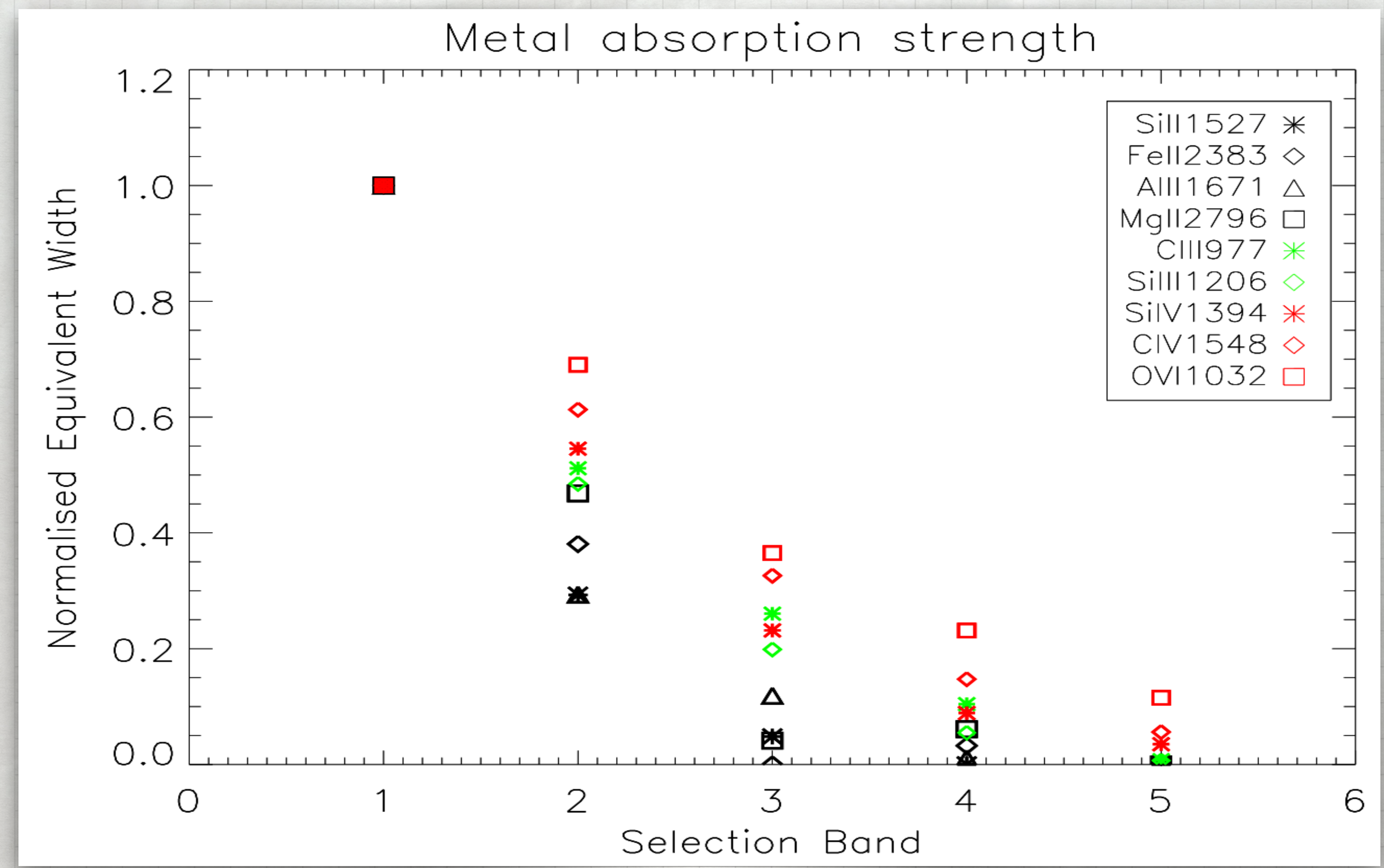

Measuring the Lyman-series lines

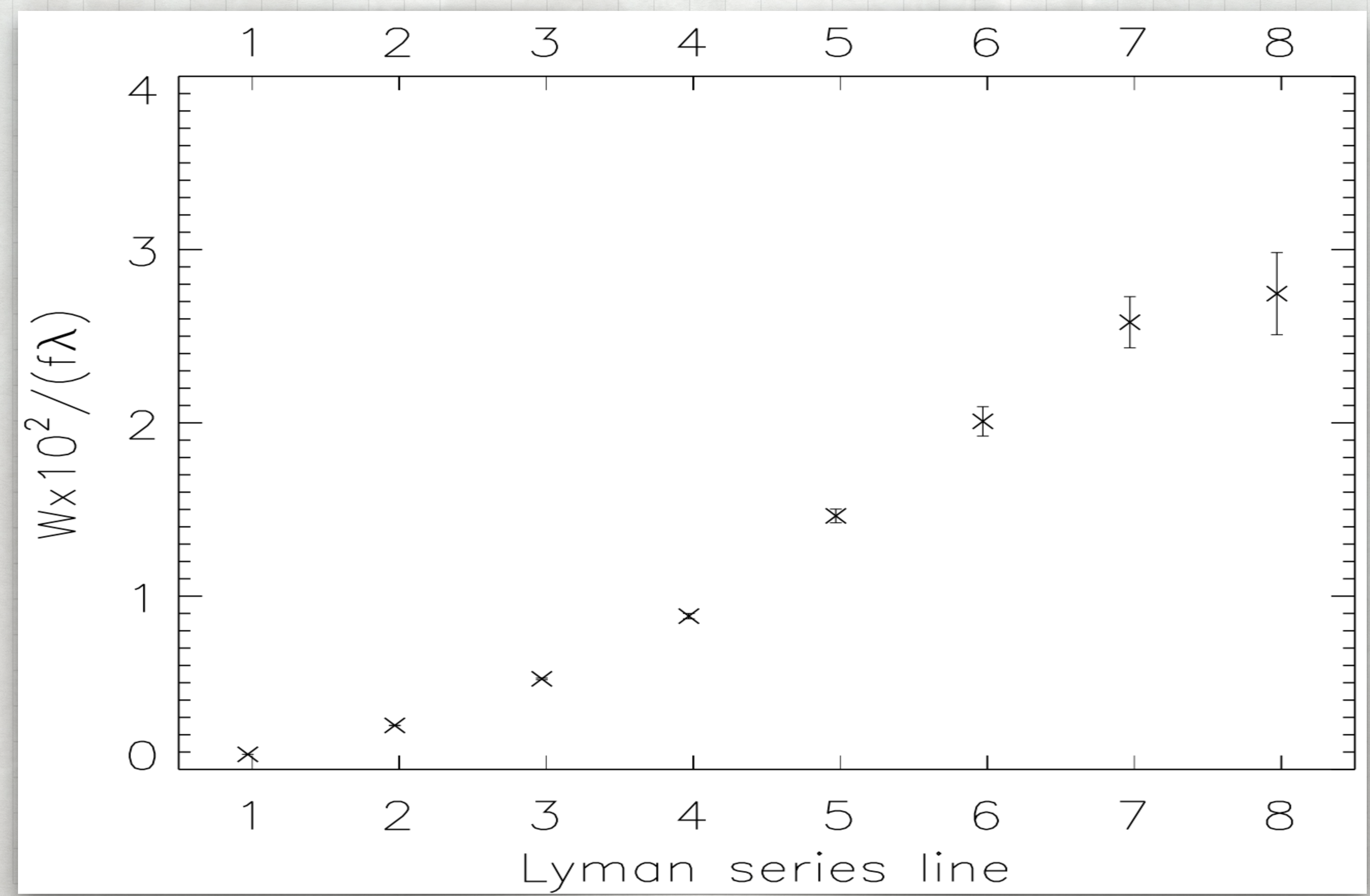

Measuring the Lyman-series lines

- Measured equivalent widths compared with single-component models

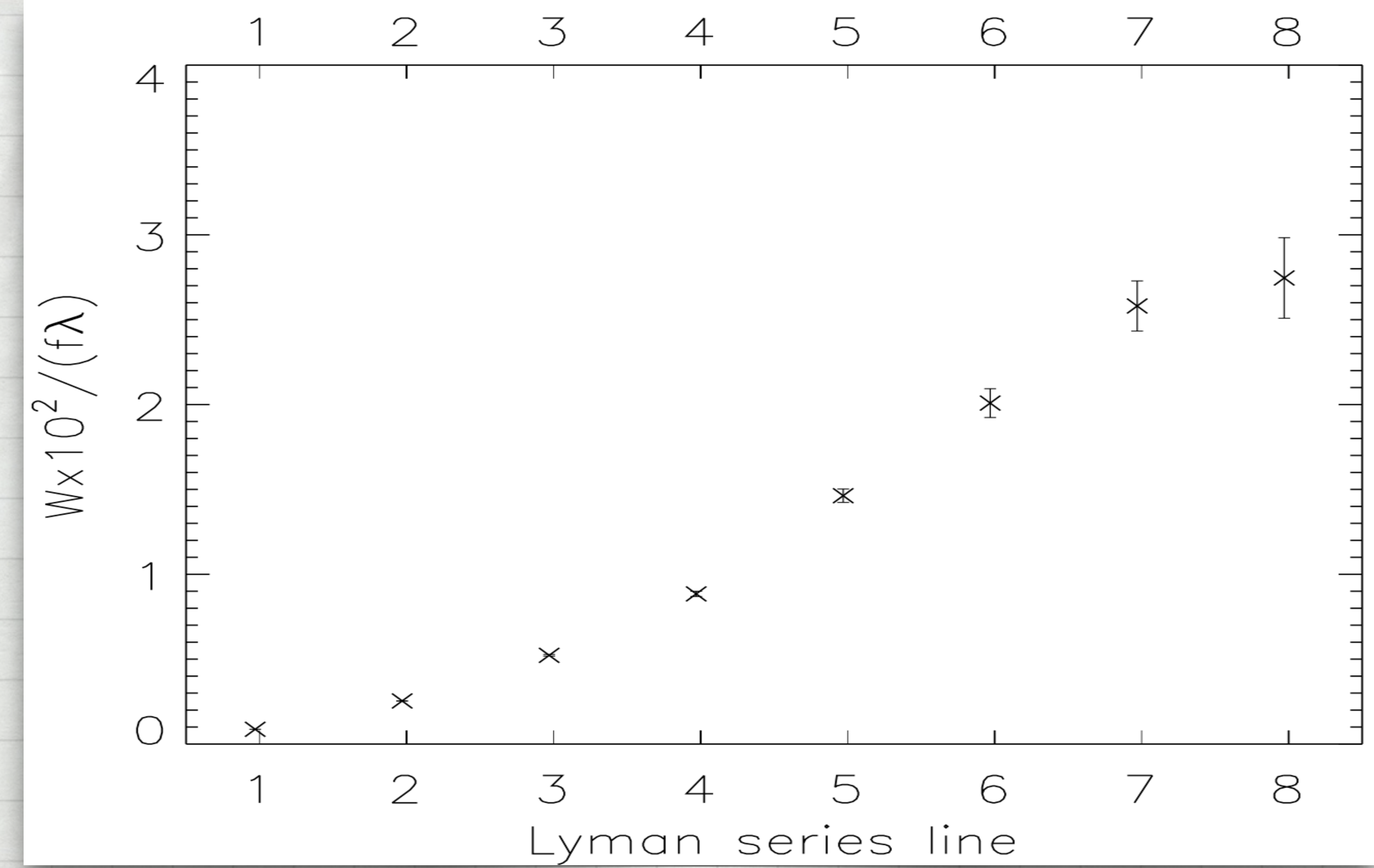

- log N_{HI} grid in [13.0,21.0]
  resolution: 0.01 cm^{-2}

- b_{eff} grid in [5,50]
  resolution: 0.1 km/s

Complications due to the presence of unsaturated non-dominant absorption along with saturated dominant absorption in lower order Lyman-series lines.

This effect should disappear in higher order Lyman-series lines

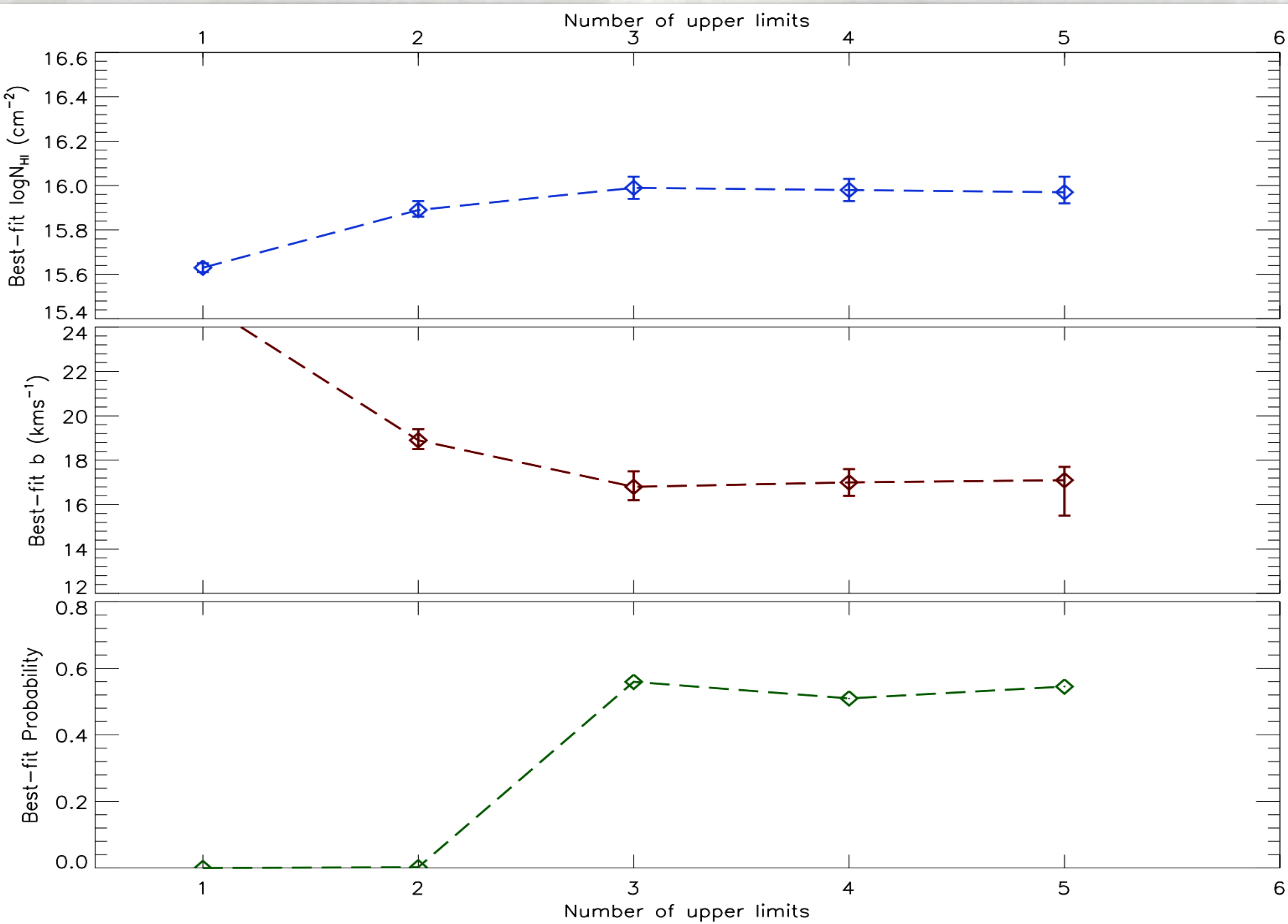
Number of upper limits
1
2
3
4
5
6
16.6
16.4
16.2
16.0
15.8
15.6
15.4
Best−fit logN$_{HI}$ (cm^{-2})
24
22
20
18
16
14
12
Best−fit b (kms^{-1})
0.8
0.6
0.4
0.2
0.0
Best−fit Probability
Number of upper limits

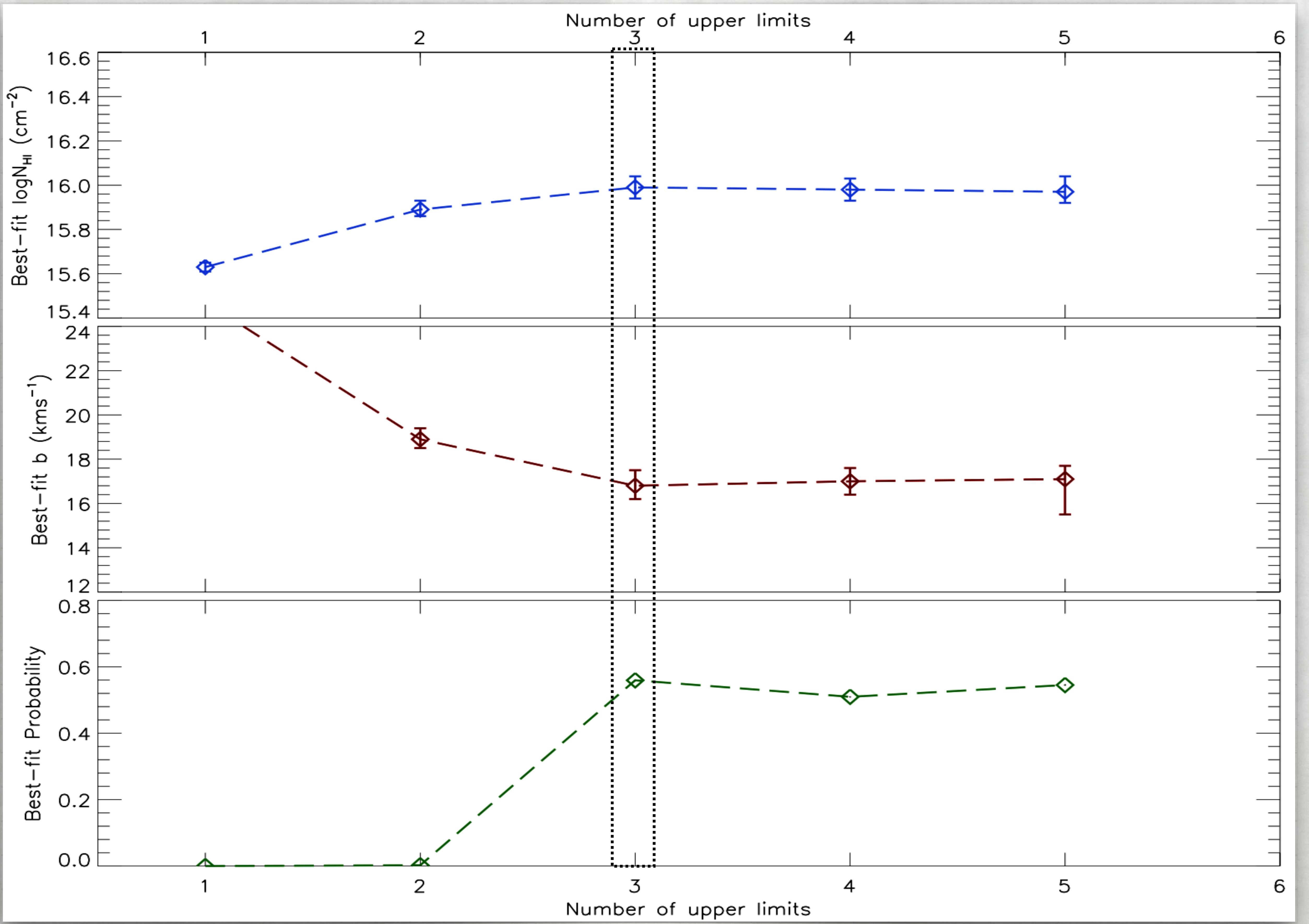

Number of upper limits
1
2
3
4
5
6
16.6
16.4
16.2
16.0
15.8
15.6
15.4
Best−fit logN$_{HI}$ (cm^{-2})
24
22
20
18
16
14
12
Best−fit b (kms^{-1})
0.8
0.6
0.4
0.2
0.0
Best−fit Probability
1
2
3
4
5
6
Number of upper limits

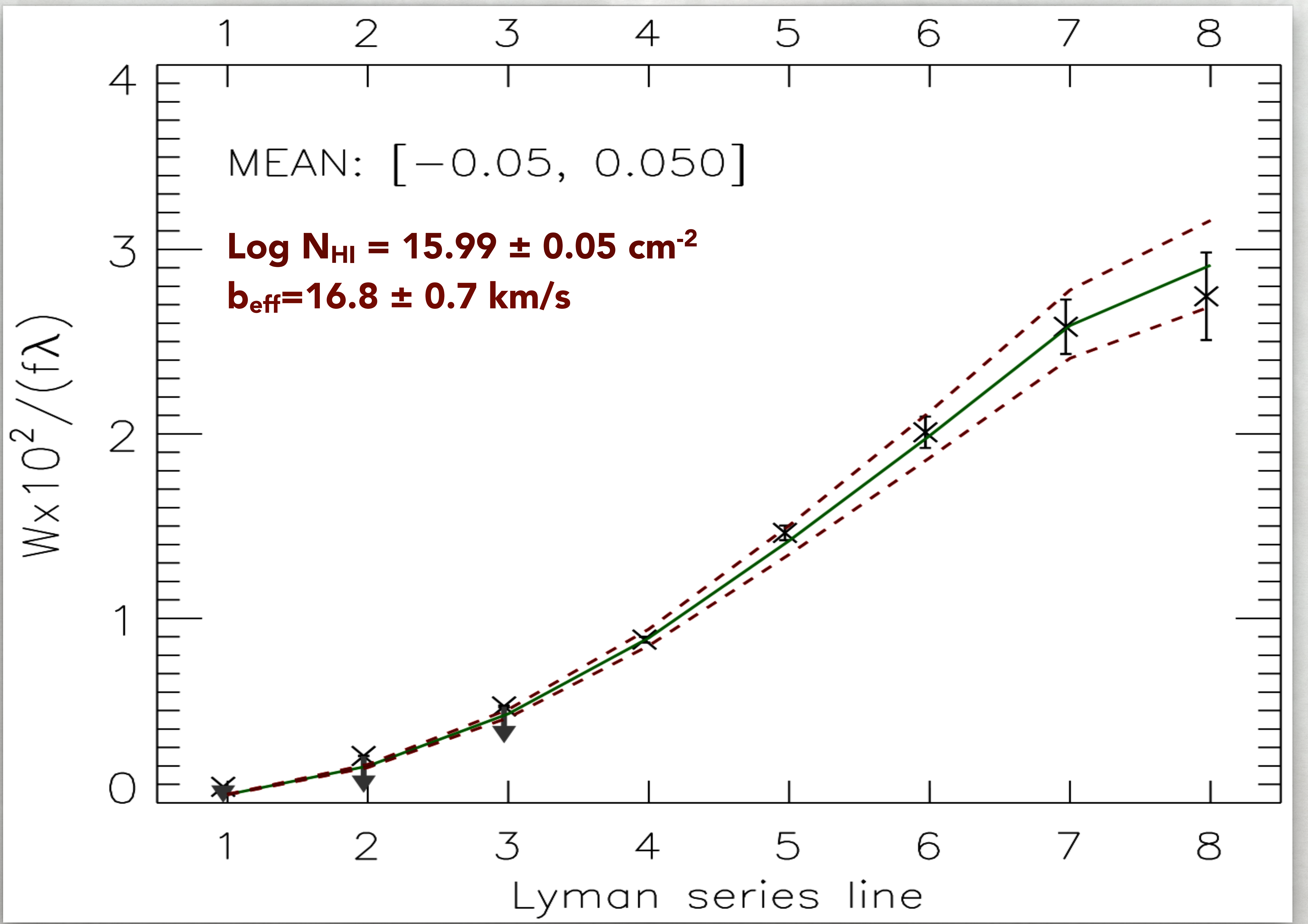
MEAN: [−0.05, 0.050]
Log N_HI = 15.99 ± 0.05 cm^-2
b_eff=16.8 ± 0.7 km/s
W×10^2/(fλ)
Lyman series line
1 2 3 4 5 6 7 8
0 1 2 3 4

Metal Column densities

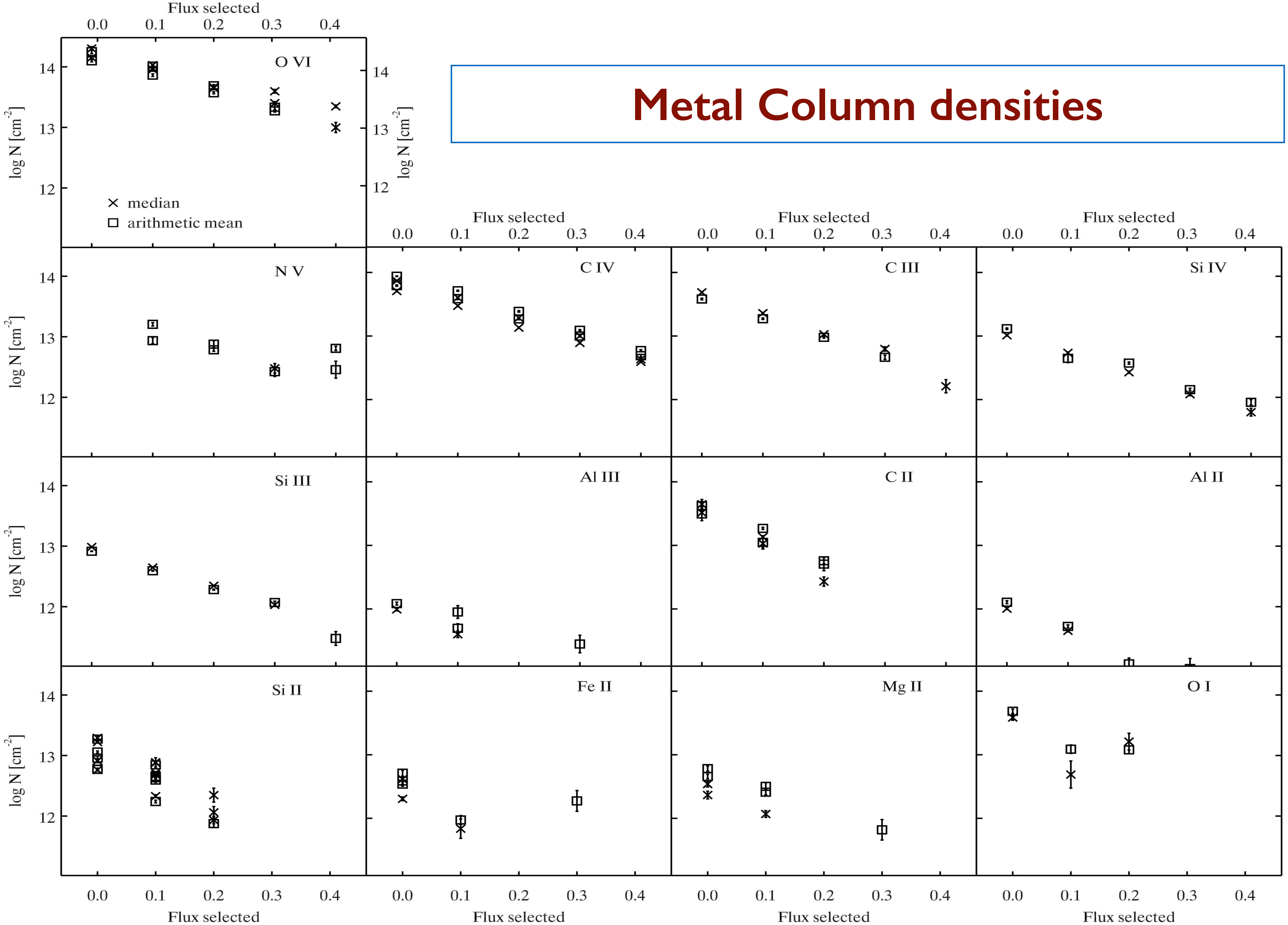

Compared with Simple Models

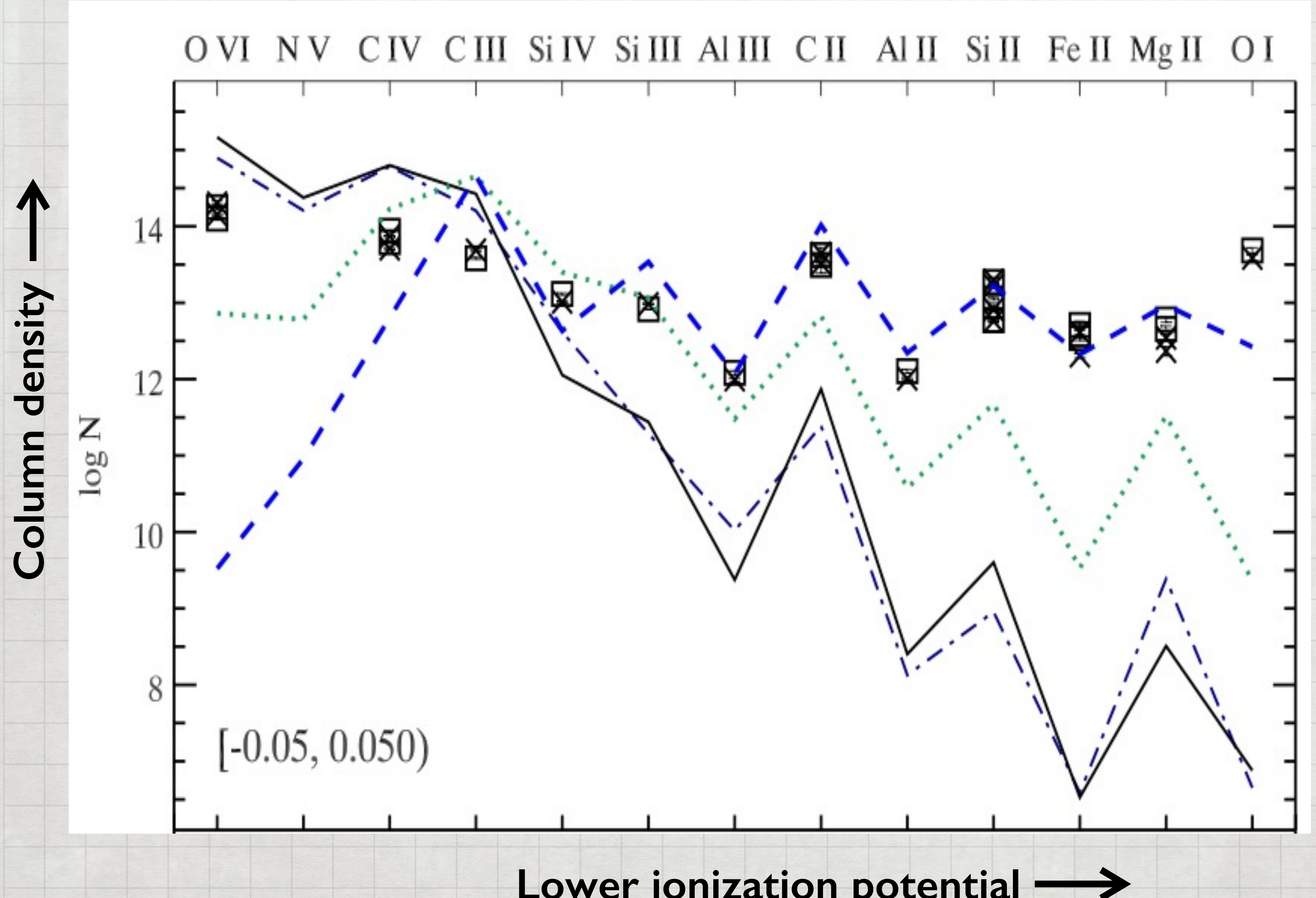

Each model constrained by measured N(H I), solar abundance, UV background @ z ~ 2.7

Compared with Simple Models

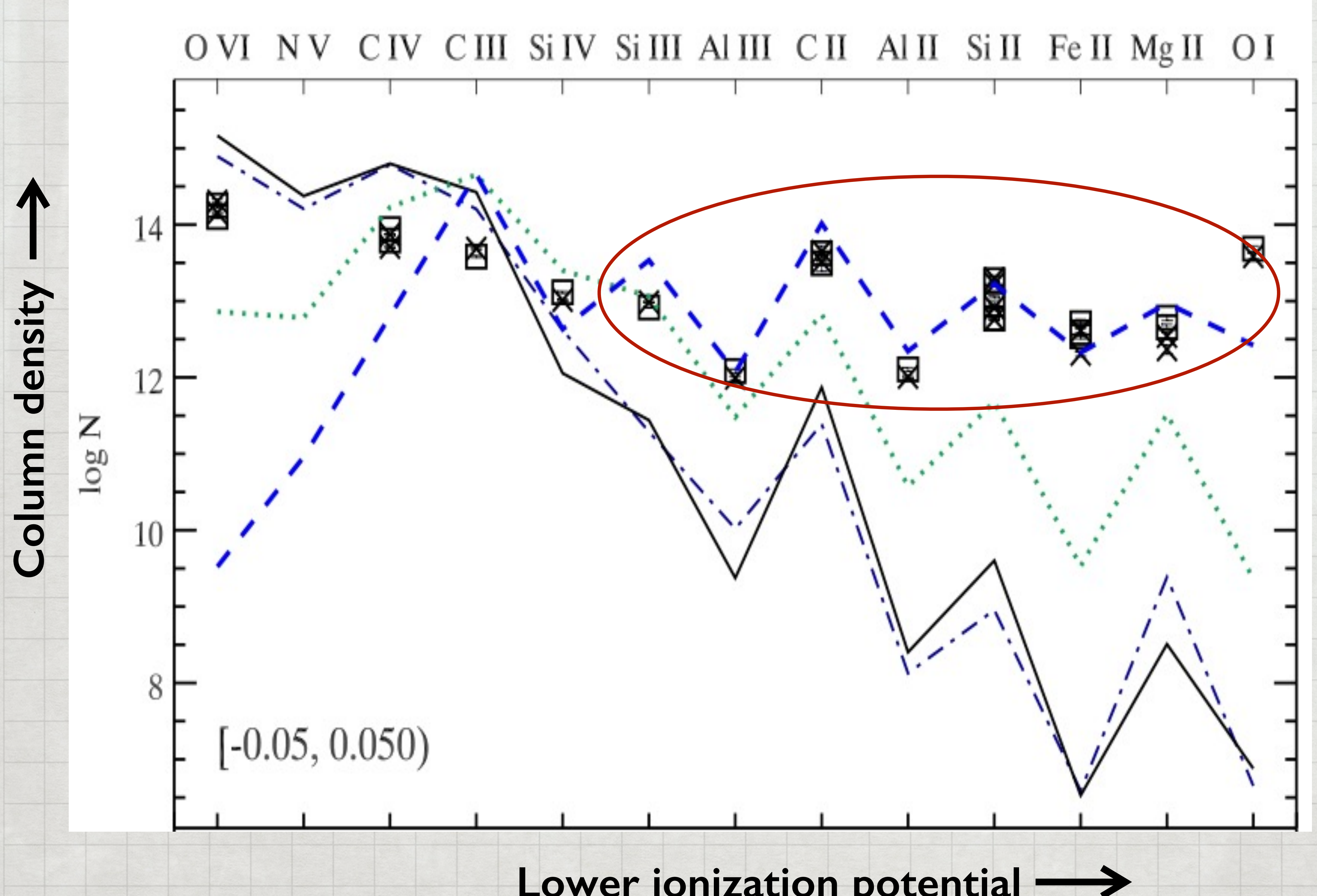

Each model constrained by measured N(H I), solar abundance, UV background @ z ~ 2.7

Compared with Simple Models

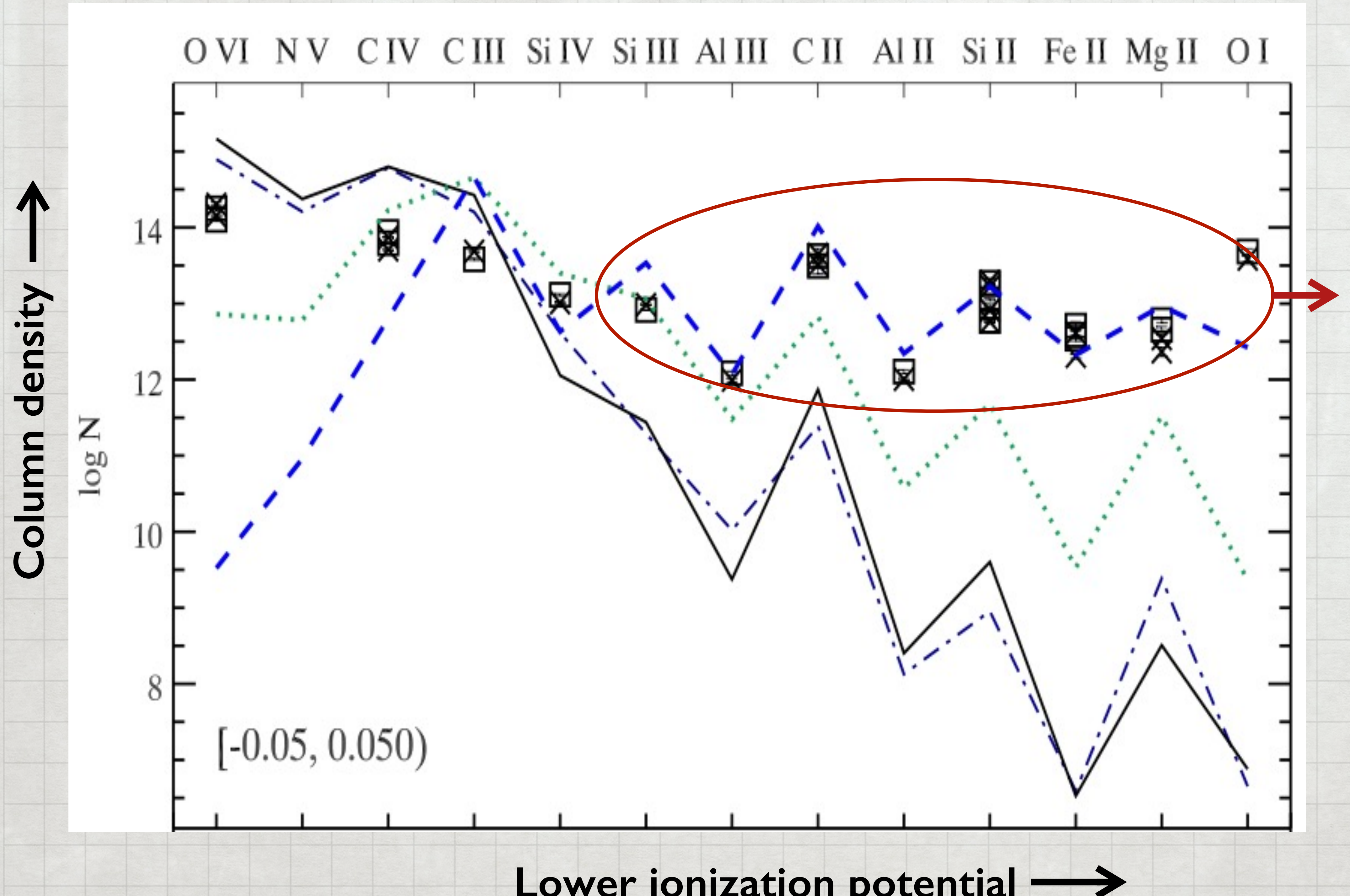

Each model constrained by measured N(H I), solar abundance, UV background @ z ~ 2.7

Compared with Simple Models

Column density ⟶

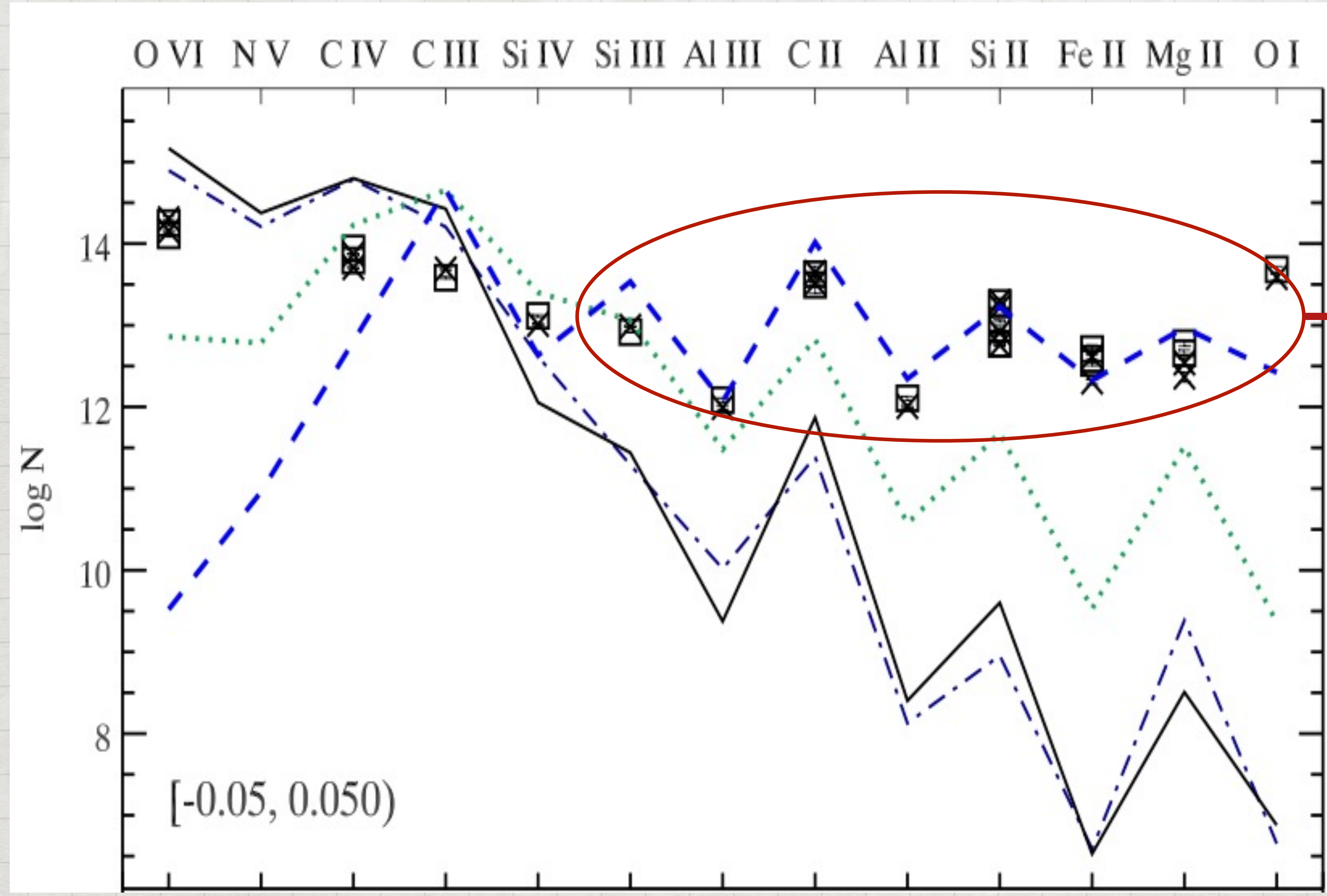

[X/H] ~ -0.5
~100 pc scale clumping

Lower ionization potential ⟶

Each model constrained by measured N(H I), solar abundance, UV background @ z ~ 2.7

Compared with a Simple Multi-phase Model

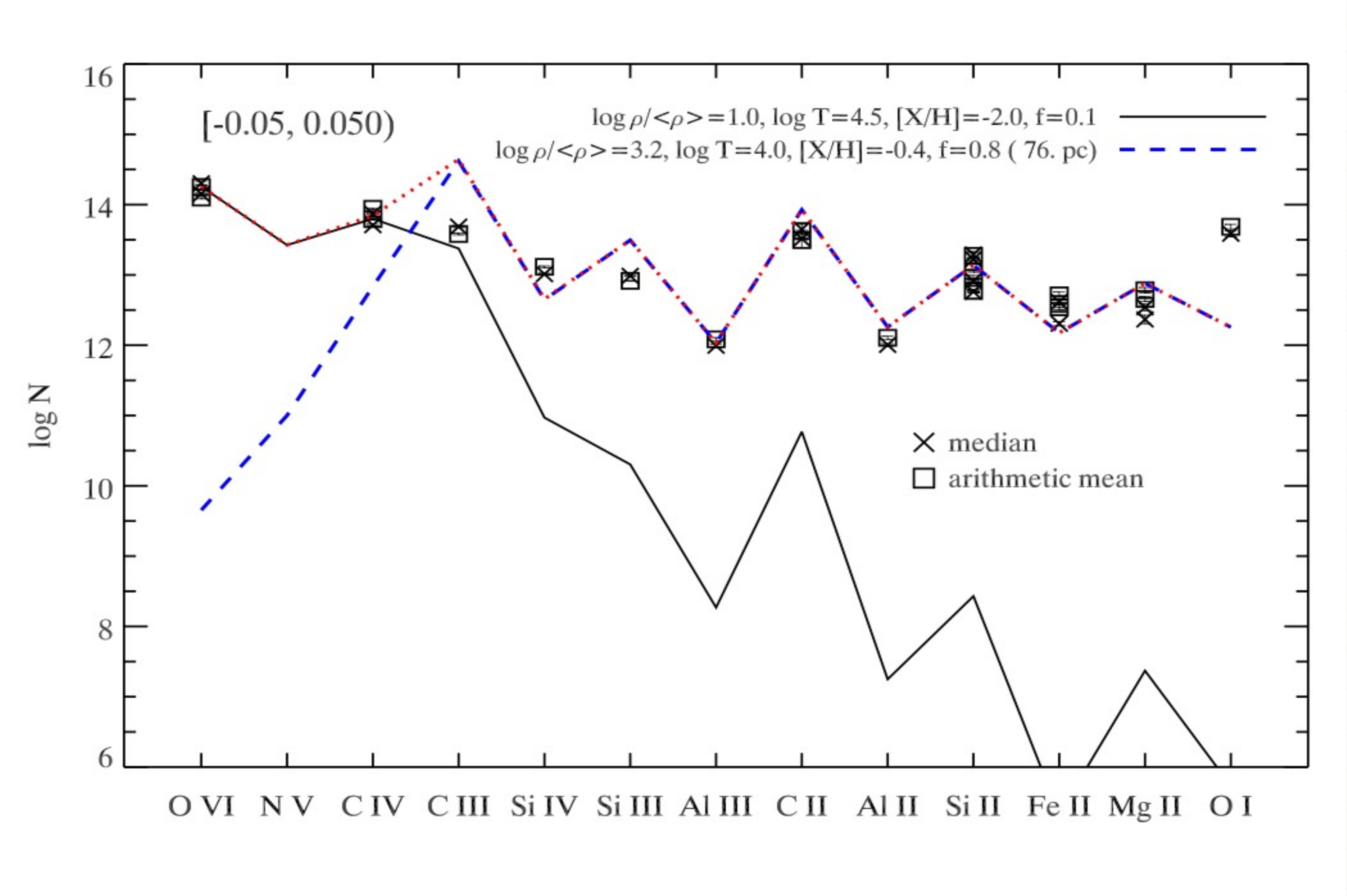

Column density →

Lower ionization potential →

Going beyond the composite: Si II absorber populations

- Populations are forward modelled
- Neighbouring pixels used as null sample
- Mean composite treated as metal target

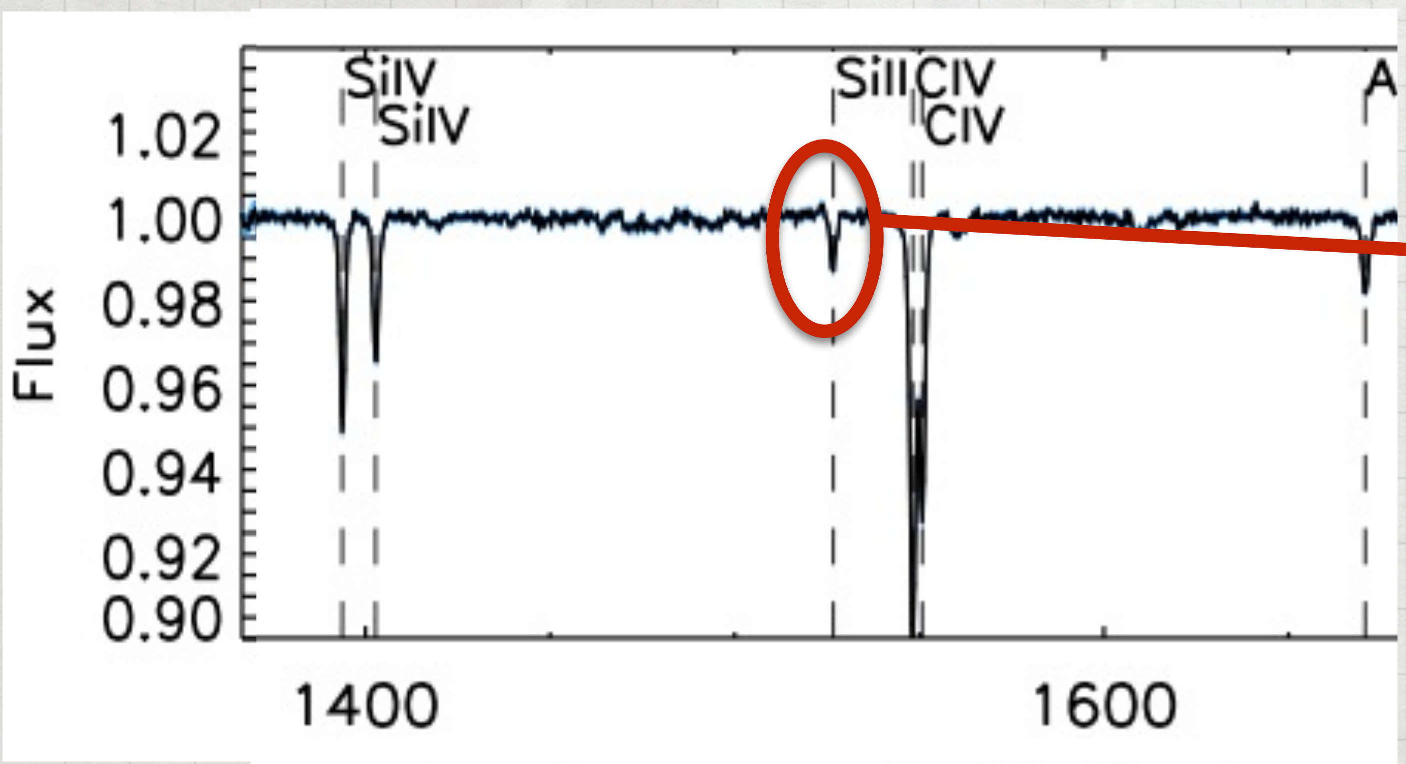

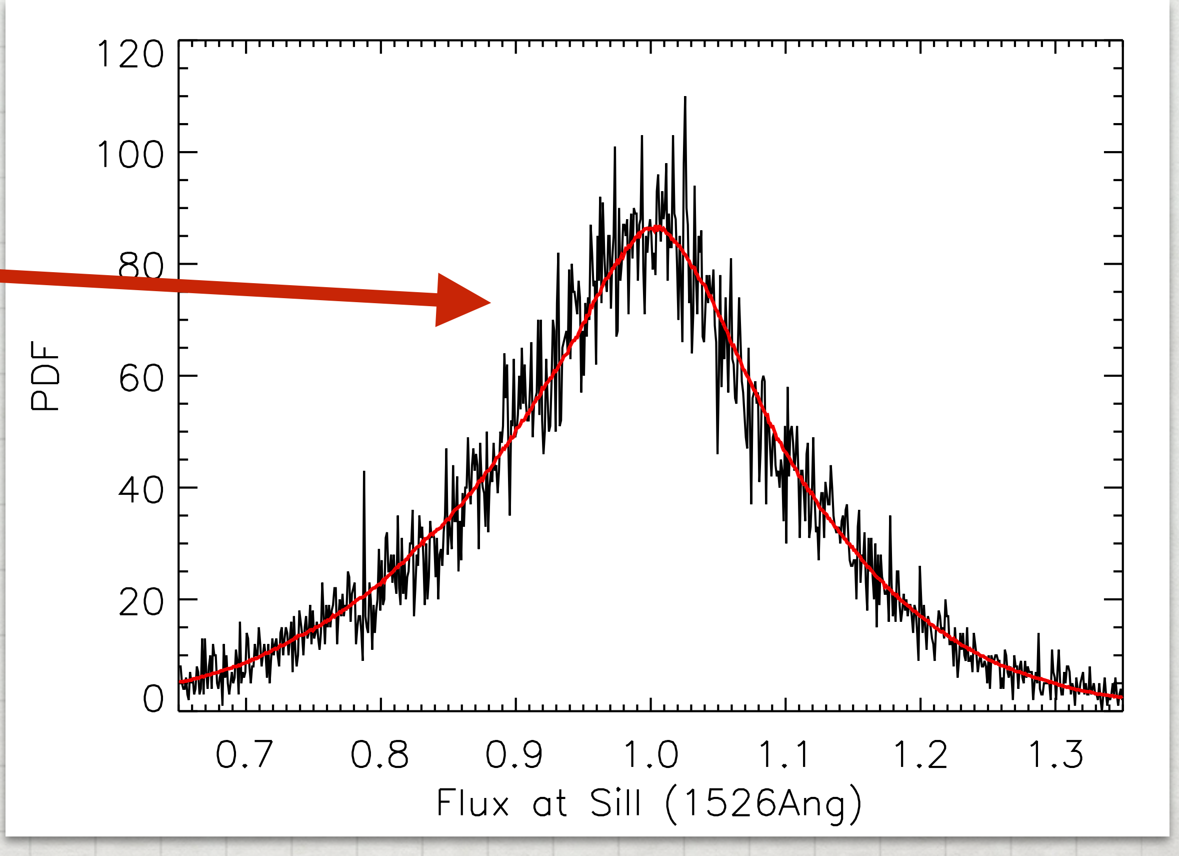

Si II sample well-modelled by *20%* population with absorption *5 x* mean (with a Gaussian scatter) and nothing elsewhere.

• Som, Pieri et al., in prep.

Going beyond the composite: Si III absorber populations

- Populations are forward modelled
- Neighbouring pixels used as null sample
- Mean composite treated as metal target

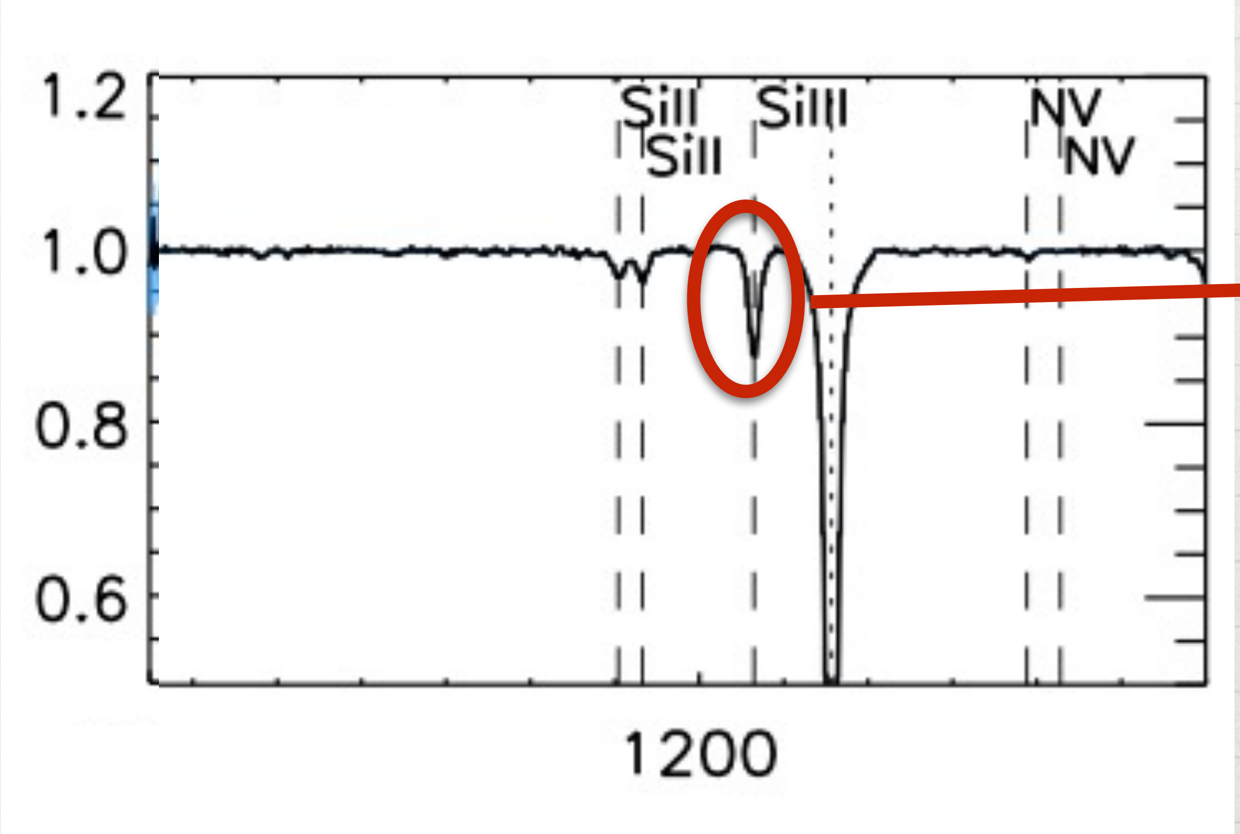

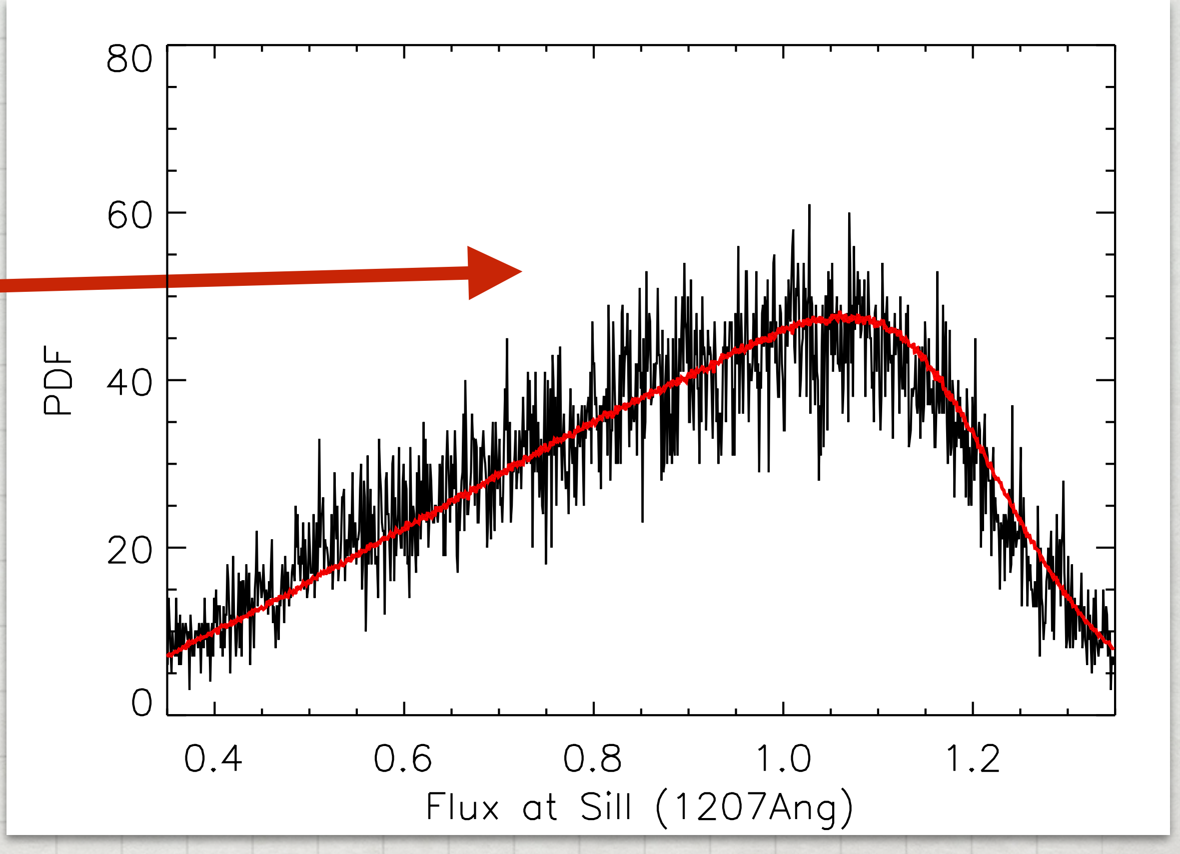

Si III sample matched by <u>*20%*</u> population 3.4 x stronger than mean. The remaining 80% also enriched.

• Som, Pieri et al., in prep.

Going beyond the composite: Si IV absorber populations

- Populations are forward modelled
- Neighbouring pixels used as null sample
- Mean composite treated as metal target

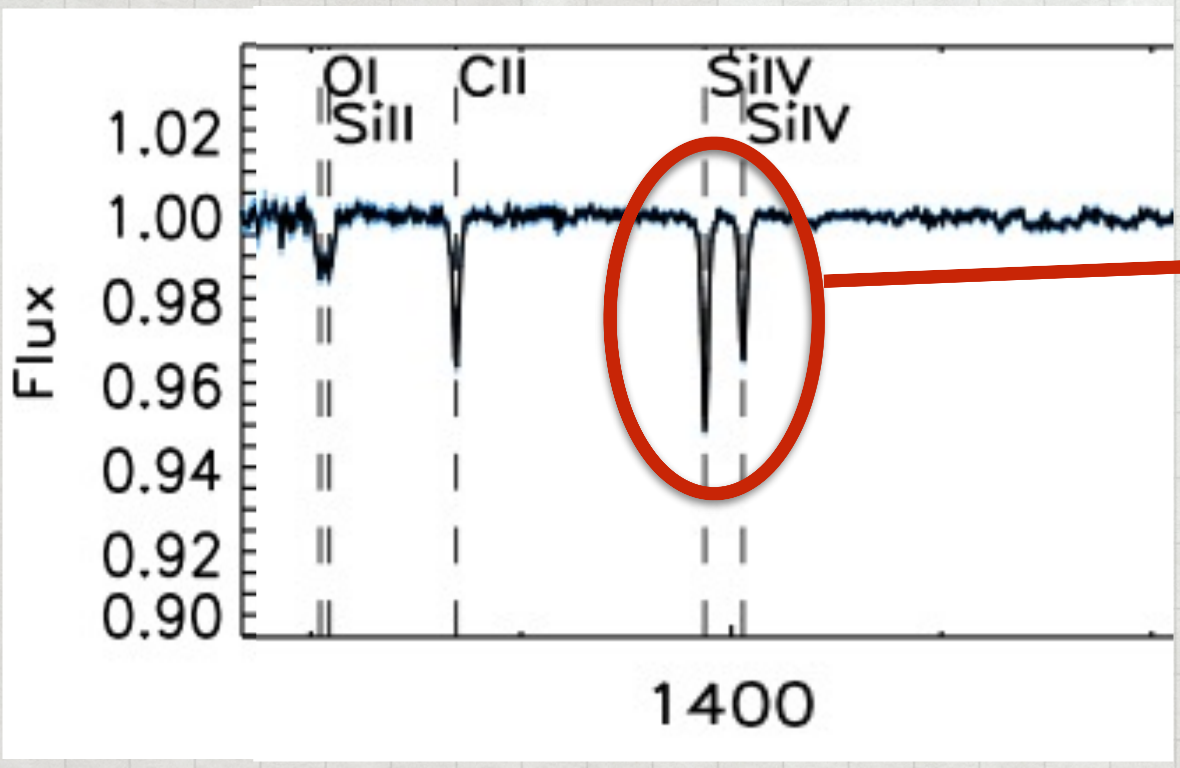

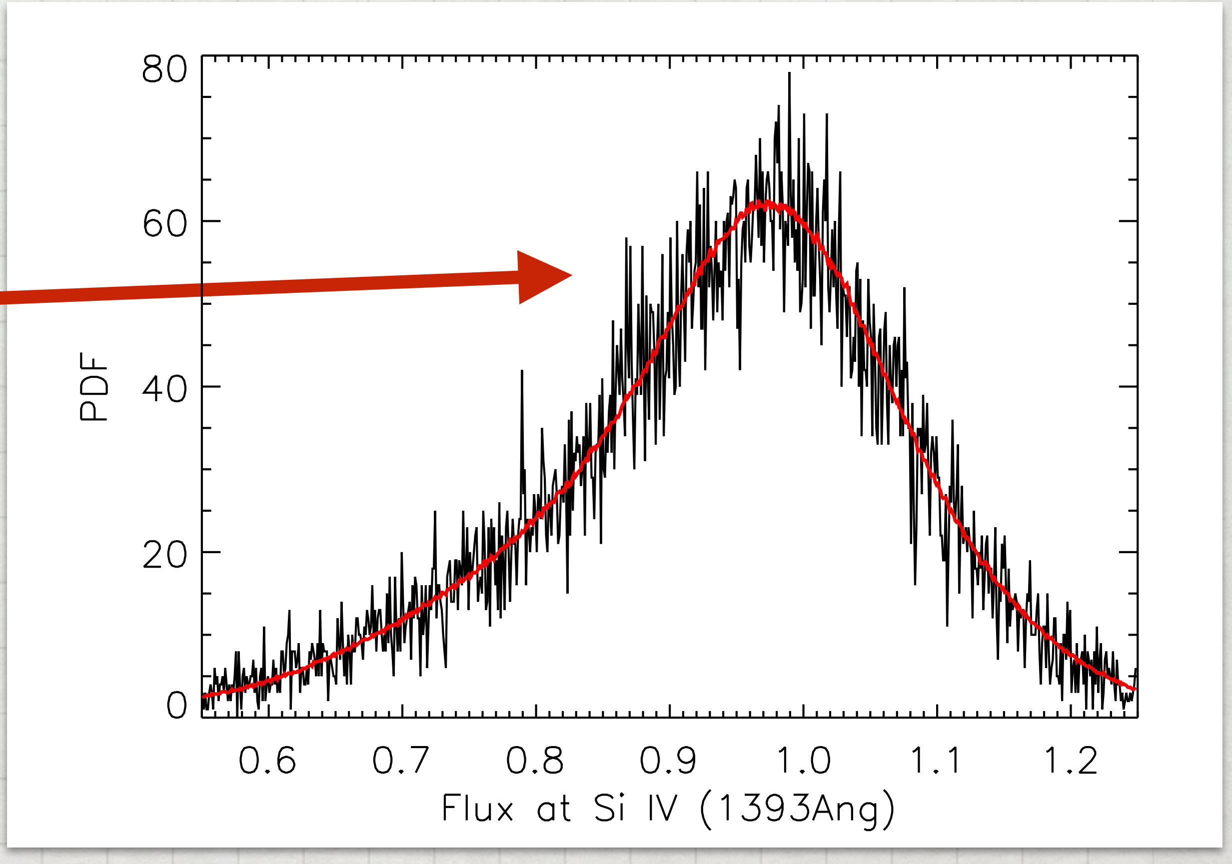

Si IV sample well matched by <u>*20%*</u> population 3.2 x stronger than mean. The remaining 80% also enriched.

• Som, Pieri et al., in prep.

Population corrected Silicon

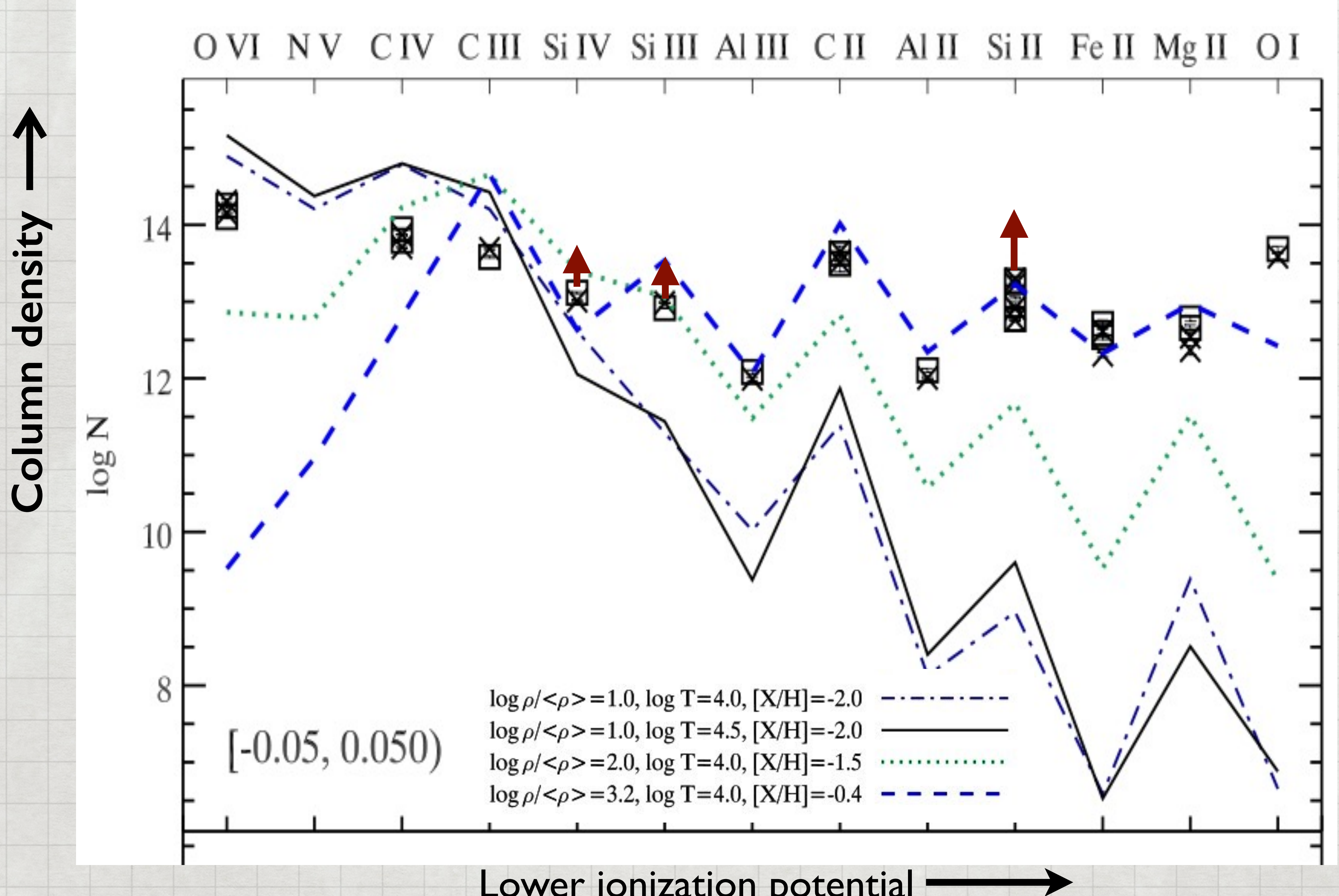

Multi population analysis → clumping scale must be even smaller and multiphase will make them smaller still

- Som, Pieri et al., in prep.

Summary

- Strong Lyman α forest lines arising in CGM regions show clustering

- Clustered strong Lyman α forest lines are blended in BOSS spectra: appropriate selection of flux decrement in BOSS spectra picks out CGM tracers (more in talks by Michael Blomqvist and Mat Pieri)

- Stacking CGM tracers retrieve the metal signal associated with the CGM regions: power of large numbers

- The picture emerging is of a clumpy, multi-phase CGM: dense, metal-rich clumps <100pc + gas at higher ionisation

Thanks!